Inorganic Chemistry

ARTICLE

pubs.acs.org/IC

Pt(II) and Pt(IV) Amido, Aryloxide, and Hydrocarbyl Complexes: Synthesis, Characterization, and Reaction with Dihydrogen and Substrates that Possess C−H Bonds

Joanna R. Webb,[†] Colleen Munro-Leighton,[⊥] Aaron W. Pierpont,[‡] Joshua T. Gurkin,[⊥] T. Brent Gunnoe,*[,†] Thomas R. Cundari,*[,‡] Michal Sabat,[§,†] Jeffrey L. Petersen,[∥] and Paul D. Boyle[⊥]

[†]Department of Chemistry, University of Virginia, Charlottesville, Virginia 22904, United States

[‡]Department of Chemistry, Center for Advanced Scientific Computing and Modeling (CASCaM), University of North Texas, Denton, Texas 76203, United States

[§]Nanoscale Materials Characterization Facility, Department of Materials Science and Engineering, University of Virginia, Charlottesville, Virginia 22904, United States

[∥]C. Eugene Bennett Department of Chemistry, West Virginia University, Morgantown, West Virginia, 26506

[⊥]Department of Chemistry, North Carolina State University, Raleigh, North Carolina 27695, United States

Supporting Information

ABSTRACT: The Pt(II) amido and phenoxide complexes (^{t}bpy)Pt(Me)(X), (^{t}bpy)Pt(X)$_2$, and [(^{t}bpy)Pt(X)(py)][BAr′$_4$] (X = NHPh, OPh; py = pyridine) have been synthesized and characterized. To test the feasibility of accessing Pt(IV) complexes by oxidizing their Pt(II) precursors, the previously reported (^{t}bpy)Pt(R)$_2$ (R = Me and Ph) systems were oxidized with I$_2$ to yield (^{t}bpy)Pt(R)$_2$(I)$_2$. The analogous reaction with (^{t}bpy)Pt(Me)(NHPh) and MeI yields the corresponding (^{t}bpy)Pt(Me)$_2$(NHPh)(I) complex. Reaction of (^{t}bpy)Pt(Me)(NHPh) and phenylacetylene at 80 °C results in the formation of the Pt(II) phenylacetylide complex (^{t}bpy)Pt(Me)(C≡CPh). Kinetic studies indicate that the reaction of (^{t}bpy)Pt(Me)(NHPh) and phenylacetylene occurs via a pathway that involves [(^{t}bpy)Pt(Me)(NH$_2$Ph)][TFA] as a catalyst. The reaction of H$_2$ with (^{t}bpy)Pt(Me)(NHPh) ultimately produces aniline, methane, ^{t}bpy, and elemental Pt. For this reaction, mechanistic studies reveal that 1,2-addition of dihydrogen across the Pt−NHPh bond to initially produce (^{t}bpy)Pt(Me)(H) and free aniline is catalyzed by elemental Pt. Heating the cationic complexes [(^{t}bpy)Pt(NHPh)(py)][BAr′$_4$] and [(^{t}bpy)Pt(OPh)(py)][BAr′$_4$] in C$_6$D$_6$ does not result in the production of aniline and phenol, respectively. Attempted synthesis of a cationic system analogous to [(^{t}bpy)Pt(NHPh)(py)][BAr′$_4$] with ligands that are more labile than pyridine (e.g., NC$_5$F$_5$) results in the formation of the dimer [(^{t}bpy)Pt(μ-NHPh)]$_2$[BAr′$_4$]$_2$. Solid-state X-ray diffraction studies of the complexes (^{t}bpy)Pt(Me)(NHPh), [(^{t}bpy)Pt(NH$_2$Ph)$_2$][OTf]$_2$, (^{t}bpy)Pt(NHPh)$_2$, (^{t}bpy)Pt(OPh)$_2$, (^{t}bpy)Pt(Me)$_2$(I)$_2$, and (^{t}bpy)Pt(Ph)$_2$(I)$_2$ are reported.

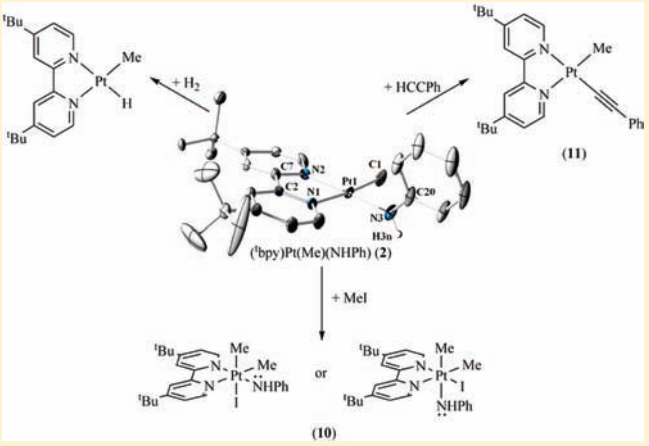

INTRODUCTION

Late transition metal centers with high d-electron counts bearing heteroatomic ligands (e.g., amido, alkyl/aryloxo, hydroxo, imido, or oxo ligands) exhibit diverse reactivity.[1−5] Such systems have been implicated in metal-mediated reactions such as olefin and alkyne hydroamination, olefin insertions, aryl amination, aryl etheration, and C−H bond activation.[2,4,6−17] The range of reactivity of these systems has been attributed, at least in part, to the disruption of ligand-to-metal π bonding.[3] Limiting ligand-to-metal π donation by using late transition metals with high d-electron counts serves to localize negative charge density on the heteroatomic ligand (i.e., compared to systems with empty dπ orbitals), imparting nucleophilic and basic reactivity.[2,3,12,13,18−21] Such reactive ligands positioned adjacent to Lewis acidic metal centers provide an opportunity to activate relatively unreactive organic substrates.

In order to identify the factors that control transformations of M−X moieties (X = NR$_2$, OR; M = high d-electron count transition metal), well-defined systems with varied oxidation states, ligand sets, metal centers, and coordination environments must be

Received: January 24, 2011
Published: March 28, 2011

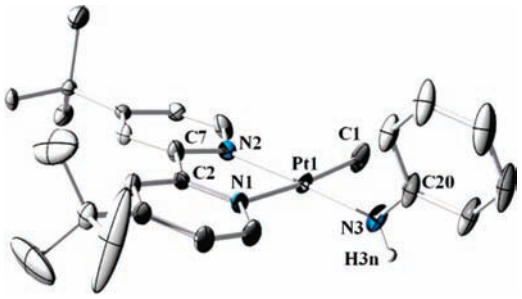

Figure 1. ORTEP diagram (50% probability) of (^{t}bpy)Pt(Me)(NHPh) (**2**) (most hydrogen atoms omitted for clarity). Selected bond lengths (Å): Pt1−N1 2.077(2), Pt1−N2 2.026(2), Pt1−C1 2.040(3), Pt1−N3 2.005(2), N3−C20 1.357(4). Selected bond angles (deg): N3−Pt1−C1 89.25(11), N2−Pt1−C1 97.26(11), N3−Pt1−N1 94.55(9), N2−Pt1−N1 78.91(9), Pt1−N3−C20 126.1(2).

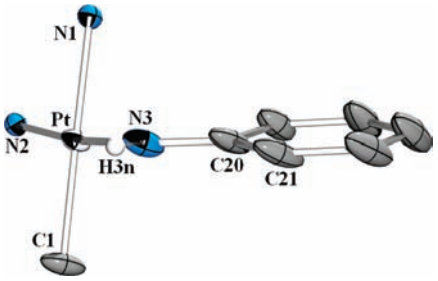

Figure 2. View of complex **2** showing that the amido orientation likely allows overlap of the N3 lone pair with the π^* system of the phenyl ring.

accessed.[22,23] Herein, we report the synthesis and characterization of neutral and cationic Pt(II) and Pt(IV) complexes with NHR or OR ligands bearing the bidentate ligand 4,4′-di-*tert*-butyl-2,2′-dipyridyl (^{t}bpy), including solid-state X-ray diffraction studies and details of the reactivity of these complexes with substrates that possess covalent bonds (i.e., H−H and C−H). Portions of this work have been previously communicated.[24]

RESULTS AND DISCUSSION

Synthesis and Characterization of Pt(II) Complexes. The labile nature of the trifluoroacetate (TFA) ligand of the previously reported complex (^{t}bpy)Pt(Me)(TFA)[25] allows coordination of aniline to afford [(^{t}bpy)Pt(Me)(NH_2Ph)][TFA] (**1**) (eq 1). A singlet with Pt satellites ($^2J_{Pt-H}$ = 70 Hz) in the ^{1}H NMR spectrum at 0.84 ppm and one at −10.4 ppm ($^1J_{Pt-C}$ = 774 Hz) in the ^{13}C NMR spectrum confirm the presence of the methyl ligand. Deprotonation with 1 equiv of Na[N($SiMe_3$)$_2$] cleanly provides the corresponding amido complex, (^{t}bpy)Pt(Me)(NHPh) (**2**) (eq 2), with a significant upfield shift of the N*H* resonance from 7.72 ppm for **1** to 3.99 ppm for complex **2**. The downfield region of the ^{1}H NMR spectrum of complex **2** is consistent with $N_{amido}-C_{phenyl}$ bond rotation that is rapid on the NMR time scale with one resonance each for the ortho and meta positions of the amido phenyl group. For **2**, the methyl group resonates as a singlet (1.85 ppm) with Pt satellites ($^2J_{Pt-H}$ = 84 Hz) in the ^{1}H NMR spectrum and −14.2 ppm ($^1J_{Pt-C}$ = 813 Hz) in the ^{13}C NMR spectrum. Complex **2** has been characterized by single-crystal X-ray diffraction and exhibits a pseudo square planar coordination sphere (Figure 1). The $Pt-N_{amido}$ bond length of **2** is 2.005(2) Å. With a Pt−N3−C20−C21 dihedral angle of 9.0(4)°, the amido lone pair is approximately aligned for donation into the π^* orbitals of the phenyl ring (Figure 2). Consequently, the $N_{amido}-C_{phenyl}$ bond length for complex **2** is 1.357(4) Å. Cowan and Trogler et al. reported the crystal structure for *trans*-PtH(NHPh)(PEt_3)$_2$ with a Pt(II)−N bond distance longer than that of **2** {2.125(5) versus 2.005(2) Å} and a shorter $N_{amido}-C_{phenyl}$ bond than that of **2** {1.343(8) versus 1.357(4) Å}.[17] Gomez et al. reported a monomeric Pt(II)-substituted amido complex, *trans*-[PtCl{NH(*p*-IC_6H_4)}(PEt_3)$_2$], with a Pt−N bond distance of 2.006(4) Å.[26]

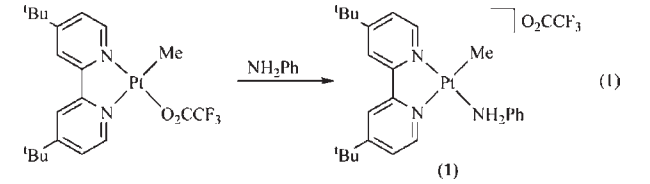

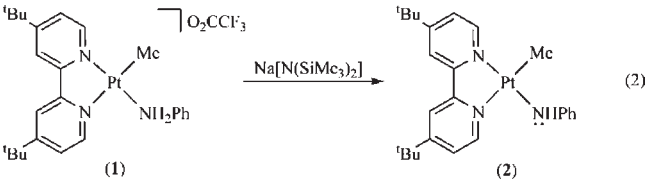

The synthesis of [(^{t}bpy)Pt(NH_2Ph)$_2$][OTf]$_2$ (**3**) was accomplished by combining excess aniline with the previously reported (^{t}bpy)Pt(OTf)$_2$ complex (eq 3).[25] Complex **3** is characterized by a broad singlet at 7.65 ppm, which integrates for four protons, due to the amine-NH_2 as well as resonances due to symmetry-equivalent pyridyl groups of the ^{t}bpy ligand in the ^{1}H and ^{13}C NMR spectra. The solid-state structure of complex **3** has been determined from a single-crystal X-ray diffraction study. Complex **3** displays no hydrogen bonding between the anilido protons and triflate counterions. The $Pt-N_{amine}$ bond lengths are 2.070(6) and 2.065(6) Å (Figure 3) and, thus, are elongated by ∼0.06−0.07 Å relative to the $Pt-N_{amido}$ bond distance of **2**. Vedernikov et al. reported a monomeric Pt(II) aniline complex, (dpms)Pt(Ph)(NH_2Ph) {dpms = di(2-pyridyl)methanesulfonate}, with a $Pt-N_{amine}$ bond length of 2.066(3) Å.[27] Radlowski et al. reported a Pt(II) complex with two chelating amine ligands with the lengths of the four Pt−N bonds between 2.023(9) and 2.073(9) Å.[28]

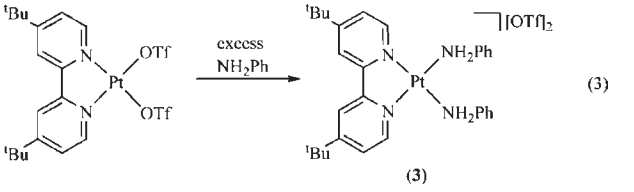

Deprotonation of both amine ligands of complex **3** with 2 equiv of Na[N($SiMe_3$)$_2$] provides the corresponding bis-amido complex (^{t}bpy)Pt(NHPh)$_2$ (**4**) (eq 4). Consistent with complexes **1** and **2**, upon deprotonation of complex **3** the N*H* resonance shifts upfield from 7.65 to 3.80 ppm. Complex **4** is also characterized by equivalent ^{t}bpy resonances in the ^{1}H and ^{13}C NMR spectra. Complex **4** crystallizes as a monomeric complex from a solution of methylene

dx.doi.org/10.1021/ic200153n |*Inorg. Chem.* 2011, 50, 4195–4211

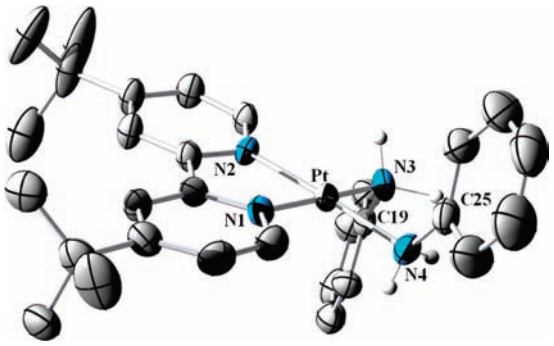

Figure 3. ORTEP diagram (50% probability) of $[(^t\text{bpy})\text{Pt}(\text{NH}_2\text{Ph})_2][\text{OTf}]_2$ (**3**) (most hydrogen atoms and the OTf counterions are omitted for clarity). Selected bond lengths (Å): Pt−N1 2.008(5), Pt−N2 2.015(5), Pt−N3 2.070(6), Pt−N4 2.065(6), N3−C19 1.468(8), N4−C25 1.474(9). Selected bond angles (deg): N1−Pt−N2 80.9(2), N1−Pt−N4 95.4(3), N2−Pt−N3 95.2(2), N4−Pt−N3 88.4(3), Pt−N4−C25 117.8(4), Pt−N3−C19 116.5(4).

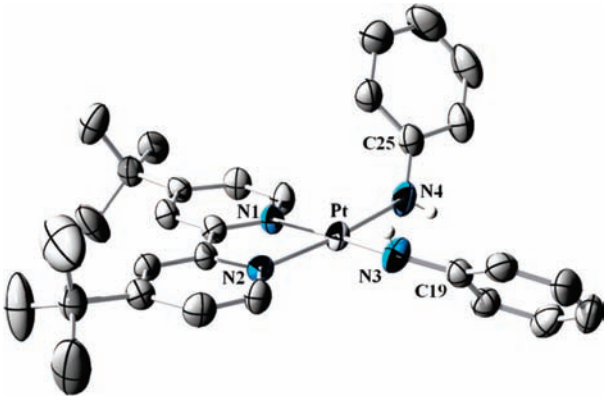

Figure 4. ORTEP diagram (50% probability) of $(^t\text{bpy})\text{Pt}(\text{NHPh})_2$ (**4**) (most hydrogen atoms omitted for clarity). Selected bond lengths (Å): Pt−N1 2.024(4), Pt−N2 2.014(4), Pt−N3 1.995(4), Pt−N4 1.984(5), N3−C19 1.362(6), N4−C25 1.371(7). Selected bond angles (deg): N4−Pt−N3 92.5(2), N3−Pt−N2 93.28(2), N4−Pt−N1 94.8(2), N2−Pt−N1 79.35(2), Pt−N4−C25 129.2(4), Pt−N3−C19 130.7(4).

chloride and hexanes. Selected bond distances and angles and the structure of **4** are shown in Figure 4. The $\text{Pt}-\text{N4}_{\text{anilido}}$ bond length for complex **4** is 1.984(5) Å, which is 0.081 Å shorter than the $\text{Pt}-\text{N4}_{\text{amine}}$ bond length of the dicationic aniline complex **3**. The $\text{Pt}-\text{N4}_{\text{anilido}}$ bond length for **4** is also shorter than the 2.005(2) Å for the $\text{Pt}-\text{N}_{\text{anilido}}$ bond of complex **2**. Indeed, the N3−C19 bond length of complex **4** is 1.371(1) Å, which is shorter than 1.474(9) Å for the N−C bond distance of the dicationic aniline complex **3**.

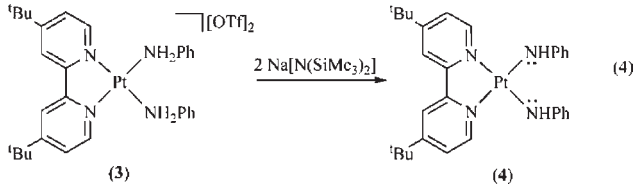

The reaction of complex **4** with 1 equiv of HCl at room temperature yields $(^t\text{bpy})\text{Pt}(\text{NHPh})(\text{Cl})$ (**5**) and free aniline (eq 5). The ^{1}H NMR spectrum of **5** reveals resonances due to inequivalent pyridyl groups of the ^{t}bpy ligand. The amido N*H* resonates as a broad singlet at 4.06 ppm, which is slightly downfield of the N*H* resonance of complex **4** (3.80 ppm).

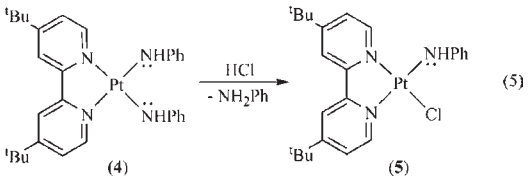

Phenoxide analogs of complexes **2** and **4** with bpy (bpy =2,2′-bipyridyl) as the supporting ligand have been reported.[29,30] The published procedure for (bpy)Pt(Me)(OPh) was used to synthesize the ^{t}bpy version.[29] Addition of excess phenol to a benzene solution of $(^t\text{bpy})\text{Pt}(\text{Me})_2$[31] results in the precipitation of $(^t\text{bpy})\text{Pt}(\text{Me})(\text{OPh})$ (**6**) (eq 6). As reported by van Koten and co-workers for (bpy)Pt(Me)(OPh), excess phenol is necessary to drive the reaction to completion, and 1 equiv of phenol is present in the isolated solid for **6** (confirmed by ^{1}H and ^{13}C NMR spectroscopy as well as elemental analysis). The methyl ligand of complex **6** resonates as a singlet at 1.00 ppm with Pt satellites ($^2J_{\text{Pt}-\text{H}}$ = 82 Hz) in the ^{1}H NMR spectrum and at −14.2 ppm ($^1J_{\text{Pt}-\text{C}}$ = 826 Hz) in the ^{13}C NMR spectrum.

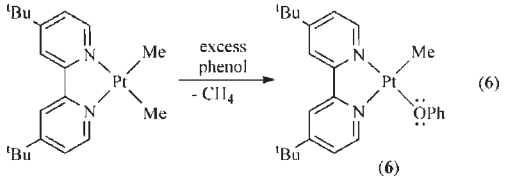

Heating a solution of complex **4** in THF with excess phenol to 80 °C yields $(^t\text{bpy})\text{Pt}(\text{OPh})_2$ (**7**) in 95% yield (eq 7). Unlike complex **6**, excess phenol can be removed from complex **7** by rinsing with copious amounts of hot hexanes. Complex **7** is characterized by aryl and ^{t}bpy resonances consistent with symmetry-equivalent pyridyl and phenoxide groups in the ^{1}H and ^{13}C NMR spectra. The solid-state structure of complex **7** has been determined by a single-crystal X-ray diffraction study (Figure 5). Complex **7** possesses a pseudosquare planar coordination geometry with angles around the platinum center falling in the range of 80.8(2)−94.5(2)°. The Pt−O bond lengths (Pt−O1 2.014(4) Å and Pt−O2 2.001(4) Å) are similar to the analogous bond length of 2.001(5) Å for the Pt−O bond of (bpy)Pt(Me)(OPh).[29] Yamamoto and co-workers reported the solid-state structure for the Pt(II) phenoxide complex *cis*-$(\text{PMe}_3)_2\text{Pt}(\text{Me})(\text{OPh})$, which has a Pt−O bond length of 2.153(9) Å, significantly longer than those of complex **7**.[32]

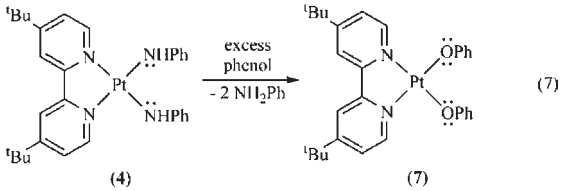

Oxidation to Pt(IV). Examples of monomeric Pt(IV) amido complexes are limited. Most reported Pt(IV) amido complexes have the amido incorporated into a chelating/bridging ligand or contain electron-deficient sulfonamide ligands.[33−37] Recently, our group

dx.doi.org/10.1021/ic200153n |*Inorg. Chem.* 2011, 50, 4195–4211

Table 1. Selected Crystallographic Data and Collection Parameters for (^{t}bpy)Pt(Me)(NHPh) (2), [(^{t}bpy)Pt(NH$_2$Ph)$_2$][OTf]$_2$ (3), (^{t}bpy)Pt(NHPh)$_2$ (4), and (^{t}bpy)Pt(OPh)$_2$ (7)

	(^{t}bpy)Pt(Me)(NHPh) (2)	[(^{t}bpy)Pt(NH$_2$Ph)$_2$][OTf]$_2$ (3)	(^{t}bpy)Pt(NHPh)$_2$ (4)	(^{t}bpy)Pt(OPh)$_2$ (7)
formula	$C_{25}H_{32}N_3Pt$	$C_{36}H_{46}F_7N_4O_6PtS_2$	$C_{30}H_{36}N_4Pt$	$C_{34}H_4N_2O_3Pt$
mol wt	569.63	1022.98	647.72	721.79
cryst syst	triclinic	triclinic	triclinic	triclinic
space group	$P\bar{1}$	$P\bar{1}$	$P\bar{1}$	$P\bar{1}$
a, Å	9.3230(4)	12.6369(8)	8.607(1)	9.0551(3)
b, Å	11.6735(5)	13.5447(4)	12.698(2)	11.7591(4)
c, Å	11.7514(5)	14.7681(4)	13.618(2)	14.6718(5)
α, deg	87.448(2)	114.171(1)	72.474(3)	96.155(1)
β, deg	73.626(2)	100.285(1)	72.801(3)	102.157(1)
γ, deg	67.519(2)	96.691(1)	87.372(3)	90.426(1)
V, *Å*^{3}	1130.92(8)	2217.88(17)	1354.2(4)	1517.69(9)
Z	2	2	2	2
D_{calcd}, Mg m^{-3}	1.673	1.532	1.588	1.579
total reflns	40 326	24 550	18 198	10 064
unique	9335	12811	9512	4421
R	0.0316	0.0548	0.0529	0.0251
R_w	0.0605	0.1577	0.0860	0.0684

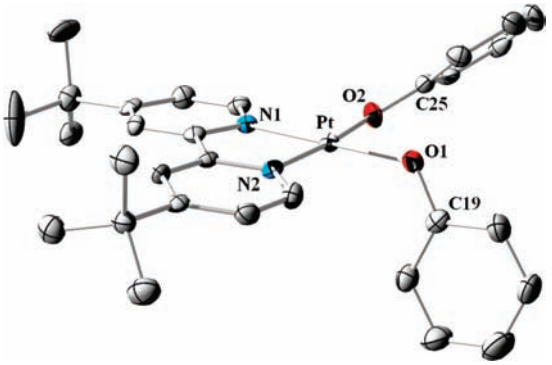

Figure 5. ORTEP diagram (50% probability) of (^{t}bpy)Pt(OPh)$_2$ (7). Selected bond lengths (Å): Pt−N2 1.988(4), Pt−N1 1.994(4), Pt−O2 2.001(4), Pt−O1 2.014(4). Selected bond angles (deg): N2−Pt−N1 80.75(2), N1−Pt−O2 91.30(2), N2−Pt−O1 94.51(2), O2−Pt−O1 93.45(2), Pt−O1−C19 124.3(3), Pt−O2−C25 127.3(3).

Table 2. Summary of Pt−methyl Coupling Constants and Anilido Chemical Shifts

	$^1J_{Pt-C}$ (Hz)	$^2J_{Pt-H}$ (Hz)	δ_{NH} (ppm)
[(^{t}bpy)Pt(Me)(NH$_2$Ph)][TFA] (**1**)	774[c]	70[a]	7.72[a]
(^{t}bpy)Pt(Me)(NHPh) (**2**)	813[b]	84[a]	3.99[a]
[(^{t}bpy)Pt(NH$_2$Ph)$_2$][OTf]$_2$ (**3**)			7.65[c]
(^{t}bpy)Pt(NHPh)$_2$ (**4**)			3.80[a]
(^{t}bpy)Pt(NHPh)(Cl) (**5**)			4.06[a]
(^{t}bpy)Pt(Me)(OPh)-HOPh (**6**)	826[b]	87[b]	
(^{t}bpy)Pt(Me)$_2$(I)$_2$ (**8**)	506[c]	73[a]	
(^{t}bpy)Pt(Me)$_2$(NHPh)(I)(**10**)	630, 642[a]	70[a]	
(^{t}bpy)Pt(Me)(CCPh) (**11**)		81[a]	
[(^{t}bpy)Pt(NHPh)(py)][BAr′$_4$] (**12**)			2.90[d]
[(^{t}bpy)Pt(*μ*-NHPh)]$_2$[BAr′$_4$]$_2$ (**14**)			2.75[c]

[a] C_6D_6. [b] Acetone-d_6. [c] $CDC1_3$. [d] CD_2Cl_2.

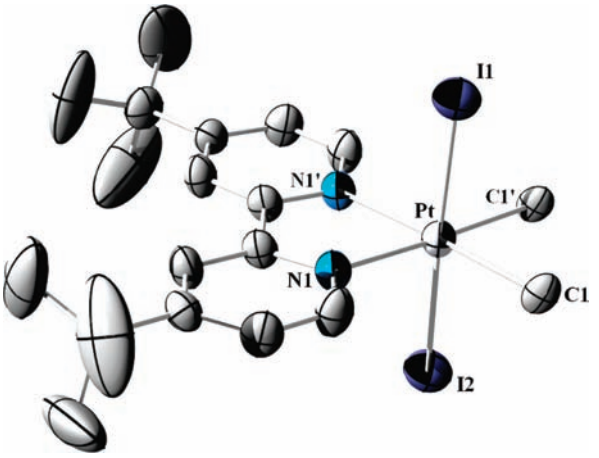

Figure 6. ORTEP diagram (50% probability) of (^{t}bpy)Pt(Me)$_2$(I)$_2$ (**8**). Selected bond lengths (Å): Pt−N1 2.168(4), Pt−C1 2.183(5), Pt−I1 2.640(1), Pt−I2 2.652(1). Selected bond angles (deg): N1−Pt−N1′ 75.5(2), N1−Pt−C1 101.1(2), C1−Pt−C1′ 82.2(3), N1−Pt−I1 91.0(1), C1−Pt−I1 88.1(2), N1−Pt−I2 89.9(1), C1−Pt−I2 91.0(2), I1−Pt−I2 178.8(2).

reported the preparation and characterization of the Pt(IV) amido complex (NCN)Pt(Me)$_2$NHPh {NCN = 2,6-(pyrazolyl-CH$_2$)$_2$-C$_6$H$_3$}.[38] We desired to prepare Pt(IV) complexes with amido and aryloxo ligands. We first tested oxidation of (^{t}bpy)Pt hydrocarbyl complexes with I$_2$.[39]

The reaction of (^{t}bpy)Pt(Me)$_2$[31] in benzene with iodine cleanly produces the Pt(IV) complex (^{t}bpy)Pt(Me)$_2$(I)$_2$ (**8**) (eq 8). Complex **8** exhibits a downfield shift from 2.12 to 3.21 ppm in the ^{1}H NMR spectrum for the methyl resonance compared to its Pt(II) analogue as well as a decrease in the $^2J_{Pt-H}$ (86 Hz compared to 73 Hz). The Pt−H coupling constant of 73 Hz for **8** is similar to the 70.4 Hz coupling constant reported by Templeton et al. for Tp′PtPh$_2$Me (Tp′ = hydridotris(3,5-dimethylpyrazolyl)borate).[40] The ^{13}C NMR spectrum of **8** reveals a $^1J_{Pt-C}$ of 506 Hz, similar to $^1J_{Pt-C}$ of 515 Hz for the closely related Pt(IV)−methyl complex

dx.doi.org/10.1021/ic200153n |*Inorg. Chem.* 2011, 50, 4195–4211

Table 3. Selected Crystallographic Data and Collection Parameters for (^{t}bpy)Pt(Me)$_2$(I)$_2$ (8) and (^{t}bpy)Pt(Ph)$_2$(I)$_2$ (9)

	(^{t}bpy)Pt(Me)$_2$(I)$_2$ (**8**)	(^{t}bpy)Pt(Ph)$_2$(I)$_2$ (**9**)
formula	$C_{20}H_{30}N_2PtI_2$	$C_{39}H_{43}I_2N_2Pt$
mol wt	747.35	988.64
cryst syst	orthorhombic	tetragonal
space group	*Pnma*	$P\bar{4}2_1c$
a, Å	17.074(1)	22.3179(3)
b, Å	14.267(1)	22.3179(3)
c, Å	20.097(2)	15.1244(2)
α, deg	90	90
β, deg	90	90
γ, deg	90	90
V, Å^3	4895.5(7)	7533.3(2)
Z	8	8
D_{calcd}, Mg m^{-3}	2.028	1.743
total reflns	31 526	56 514
unique reflns	5791	6514
R	0.0487	0.0232
R_w	0.1332	0.0783

(^{t}bpy)Pt(Me)$_2$(Br)$_2$.[41] The solid-state structure of complex **8** has been determined by a single-crystal X-ray diffraction study (Figure 6). The structure reveals trans iodide ligands with Pt−I bond distances of 2.640(1) and 2.652(1) Å. The unit cell contains two independent half-molecules, which each lie on a mirror plane passing through the corresponding Pt and pair of I atoms. The bond lengths and angles do not vary substantially between the two molecules. Only one molecule has been shown in Figure 6.

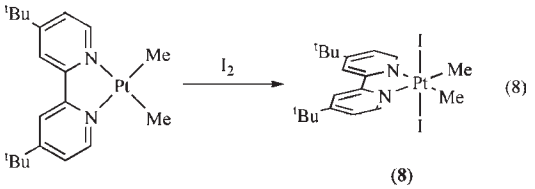

(8) (8)

A preparation similar to that for complex **8** was used for the synthesis of (^{t}bpy)Pt(Ph)$_2$(I)$_2$ (**9**) from the reaction of (^{t}bpy)Pt(Ph)$_2$ with iodine (eq 9). The solid-state structure of complex **9** was determined by a single-crystal X-ray diffraction study (Figure 7). The structure reveals trans iodide ligands and phenyl ligands that are rotated 47° (N2−Pt−C19−C20 dihedral angle) out of the square plane containing the ^{t}bpy ligand. It is unclear whether trans iodide complexes **8** and **9** are thermodynamic products or kinetic products that undergo fast isomerization.

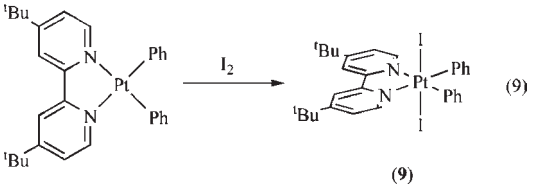

(9) (9)

With the successful conversion of Pt(II)−hydrocarbyl complexes to Pt(IV) bis-iodide systems, the oxidation of complex **2** with I_2 was attempted. In separate experiments, reactions of complex **2** with either 1 equiv or excess I_2 in various solvents (e.g., chloroform, acetone, acetonitrile, and nitromethane) resulted in incomplete

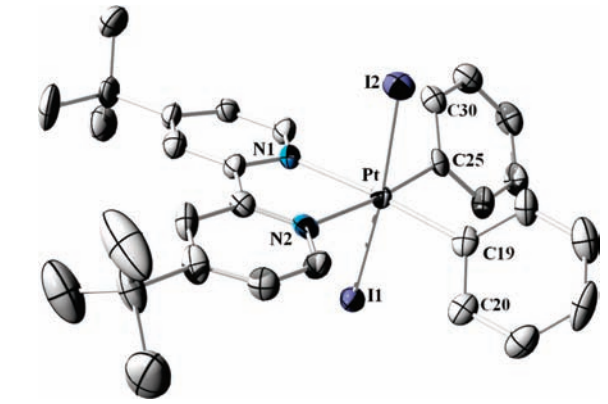

Figure 7. ORTEP diagram (50% probability) of (^{t}bpy)Pt(Ph)$_2$(I)$_2$ (**9**). Selected bond lengths (Å): Pt−C25 2.045(6), Pt−C19 2.054(7), Pt−N1 2.162(5), Pt−N2 2.173(5), Pt−I1 2.6481(5), Pt−I2 2.6598(5). Selected bond angles (deg): C25−Pt−C19 87.3(2), C25−Pt−N1 97.8(2), C19−Pt−N2 99.3(2), N1−Pt−N2 75.6(2), C25−Pt−I1 90.79(2), C19−Pt−I1 92.68(2), N1−Pt−I1 85.72(1), N2−Pt−I1 90.20(1), C25−Pt−I2 93.49(2), C19−Pt−I2 91.14(2), N1−Pt−I2 90.12(1), N2−Pt−I2 85.13(1).

conversion or decomposition to multiple products after ~20 h at room temperature. In contrast to the reaction of **2** with I_2, the reaction of complex **2** with a slight excess of iodomethane in benzene results in clean conversion to (^{t}bpy)Pt(Me)$_2$(NHPh)(I) (**10**) (eq 10). The ^{1}H NMR spectrum of **10** reveals two methyl resonances that are shifted significantly downfield (2.24 and 4.77 ppm) compared to complex **2** (1.85 ppm) as well as a downfield shift for the amido N*H* resonance from 3.99 ppm for **2** to 4.77 ppm for **10**. In comparison, the amido N*H* signal for (NCN)Pt(Me)$_2$(NHPh), also a 6-coordinate d^6 anilido complex, is observed at 2.88 ppm.[38] In addition, the conversion of **2** to **10** results in a decrease of $^2J_{Pt-H}$ for the Pt−CH$_3$ group from 84 to 70 Hz for both methyl resonances. The ^{13}C NMR spectrum of **10** also reveals a downfield shift for the methyl resonances (−14.2 ppm for complex **2** versus 13.8 and −0.4 ppm for **10**) and a decrease in coupling constant with $^1J_{Pt-C}$ = 813 Hz for complex **2** versus $^1J_{Pt-C}$ = 630 and 642 Hz for complex **10**. The ^{1}H and ^{13}C NMR spectra are consistent with a trans orientation of either the methyl/iodide or the methyl/anilido ligands, as depicted in eq 10.

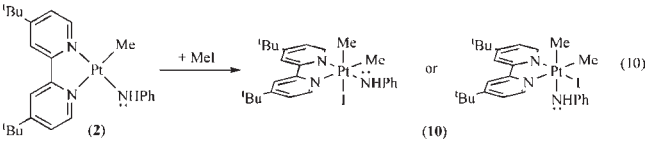

(2) (10) (10)

Reactivity with H_2 and Substrates that Possess C−H Bonds. Selective functionalization of C−H bonds is an important class of transformations because of the broad applicability to organic synthesis.[42] In general, the functionalization of C−H bonds requires two steps, C−H activation and C−X bond formation. Early transition metal−imido systems initiate C−H activation of hydrocarbons by 1,2-addition across metal−imido bonds to produce amido hydrocarbyl products.[43−47] For these reactions, detailed studies have established the importance of C−H coordination to the metal center and polarized M=NR bonds to facilitate the 1,2-addition reaction.[43,45−47] Although C−H activation has been demonstrated, C−N bond formation

dx.doi.org/10.1021/ic200153n |*Inorg. Chem.* 2011, 50, 4195–4211

via reductive coupling with these early metal complexes has not been observed, to our knowledge. Extension of the 1,2-addition reaction to late transition metal systems bearing formally anionic heteroatomic ligands might allow incorporation into a catalytic cycle for controlled C−H activation and functionalization. However, few late transition metal systems have demonstrated 1,2-CH-addition, and a more detailed understanding of the factors that control the reaction are needed.[12−14,16,22,48−50]

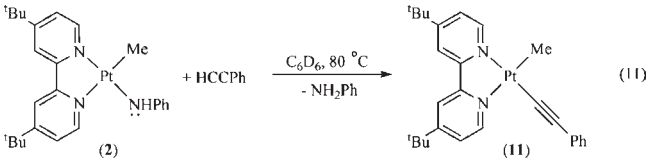

(11)

The basic and nucleophilic character of amido or alkoxide ligands coordinated to late transition metal systems in low oxidation states has been demonstrated. Previously, our group reported that TpRu(L)$_2$(X) {X = OH, NH$_2$, NH^{t}Bu, NHPh; L = PMe$_3$, P(OMe)$_3$} complexes possess nucleophilic anilido and hydroxo ligands. For example, TpRu(L)$_2$(NHPh) reacts with malononitrile (p$K_a \approx 24$ in THF)[51] at room temperature to form the ion pair [TpRu(L)$_2$-NH$_2$Ph][HC(CN)$_2$]. TpRu(L)$_2$(NHPh) does not react with phenylacetylene (p$K_a \approx 28$ in DMSO)[52] at room temperature, but upon heating at 80 °C free aniline and the phenylacetylide complexes TpRu(L)$_2$(C≡CPh) are formed (see below).[53] The combination of TpRu(L)$_2$(NHR) (R = H or ^{t}Bu) with phenylacetylene at room temperature results in the formation of a Ru−amine/acetylide ion pair, [TpRu(L)$_2$(NH$_2$R)][C≡CPh].[53] Thus, substitution of the amido phenyl substituent with H or ^{t}Bu results in a more basic amido ligand. Bergman and co-workers reported that the parent amidoruthenium complex *trans*-[(DMPE)$_2$Ru(H)(NH$_2$)] {DMPE = 1,2-bis(dimethylphosphinoethane)} reacts at room temperature with phenylacetylene to release ammonia and form the phenylacetylide complex.[19] At low temperature, the initial amido/acetylide ion pair is observed before conversion to the phenylacetylide complex. The parent amido complex is also sufficiently basic to deprotonate triphenylmethane (pK_a = 30.6 in DMSO) to form an equilibrium between the parent amido complex/triphenylmethane and the Ru−amine/triphenylmethide ion pair.[19] Related Ru(II) and Fe(II) parent amido complexes demonstrate similar acid/base reactivity.[21,54] Perhaps more germane here, two-coordinate Cu(I) complexes with amido, alkoxide, and sulfide ligands exhibit nucleophilic character at the heteroatomic ligand.[55−57]

In order to delineate metal-based effects, including d-electron count and coordination geometry, similar studies were extended to the Pt(II) systems discussed above. The Pt(II) systems are d^8 and square planar versus d^6 Ru(II) octahedral systems. The square planar geometry provides access to an empty p orbital perpendicular to the square plane, which could facilitate substrate coordination. Also, Pt(II) possesses increased electronegativity versus Ru(II) (χ = 1.513 for Pt(II) and 1.434 for Ru(II) on the Pauling scale).[58]

To directly compare the reactivity of the Pt(II) anilido systems with the systems discussed above, complex **2** was reacted with phenylacetylene. Heating a C_6D_6 solution of (^{t}bpy)Pt(Me)(NHPh) (**2**) with phenylacetylene at 80 °C results in a reaction that is complete after ∼8 h (eq 11). The ^{1}H NMR spectrum of the reaction mixture reveals the formation of free aniline and the corresponding phenylacetylide complex, (^{t}bpy)Pt(Me)(C≡CPh) (**11**), which has been isolated and characterized by ^{1}H and ^{13}C NMR spectroscopy as well as elemental

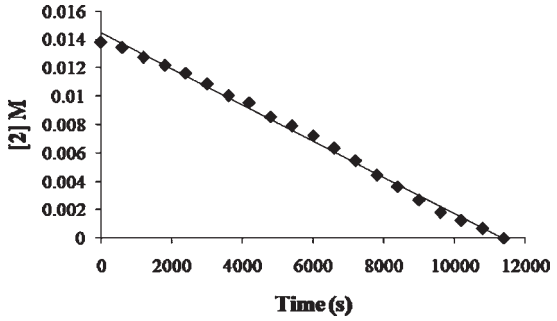

Figure 8. Plot of [**2**] versus time for the reaction of **2** with 0.112 M phenylacetylene at 80 °C (R^2 = 0.99).

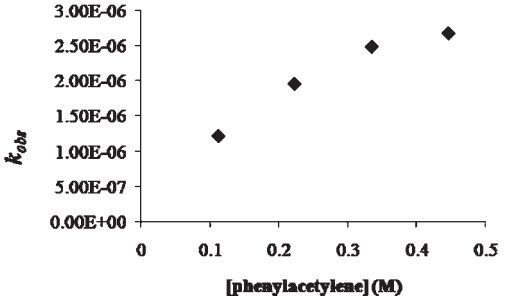

Figure 9. Plot of k_{obs} versus concentration of phenylacetylene for conversion of (^{t}bpy)Pt(Me)(NHPh) (**2**) and phenylacetylene to aniline and (^{t}bpy)Pt(Me)(C≡CPh) (**11**).

analysis. The resonance at 3.99 ppm for the amido N*H* of **2** is replaced by a broad resonance at 2.78 ppm characteristic of the free aniline N*H*$_2$ resonance along with downfield resonances consistent with the phenyl group of free aniline. In addition, the resonance for the phenylacetylene *H*−C≡CPh is absent in the ^{1}H NMR spectrum, and resonances at 103.0 and 100.6 ppm in the ^{13}C NMR spectrum are consistent with a phenylacetylide ligand. The reaction proceeds without observation of an amine−acetylide ion pair. As discussed above, *trans*-[(DMPE)$_2$Ru(H)(NH$_2$)] and TpRu(L)$_2$(NHR) (R = H or ^{t}Bu) react with phenylacetylene at room temperature[19,53] but TpRu(L)$_2$(NHPh) only reacts with phenylacetylene at 80 °C (see above).

Initial kinetic studies gave inconsistent rates for the reaction of complex **2** with phenylacetylene. For example, using two different batches of complex **2** resulted in rates differing by ∼20%, indicating the possibility that an impurity was catalyzing the reaction. Monitoring the reaction of **2** with excess phenylacetylene at 80 °C (^{1}H NMR) and plotting [**2**] versus time reveals a linear dependence, which is indicative of a zero-order dependence on complex **2** (Figure 8). Pseudo-first-order reactions of complex **2** and excess phenylacetylene concentrations (based on **2**) were run at 80 °C. A plot of k_{obs} versus phenylacetylene concentration reveals that at 0.445 M phenylacetylene the reaction rate begins to saturate (Figure 9).

With a zero-order dependence on complex **2** for the rate of conversion of **2** and phenylacetylene to **11**, the possibility that the reaction is catalyzed by a precursor to complex **2** was considered. A series of reactions of complex **2**, phenylacetylene, and varied concentrations of [(^{t}bpy)Pt(Me)(NH$_2$Ph)][TFA] (**1**), the precursor to complex **2**, were performed to investigate this possibility. A plot of k_{obs} versus equivalents of [(^{t}bpy)-Pt(Me)(NH$_2$Ph)][TFA] (**1**) reveals a linear increase in the rate

dx.doi.org/10.1021/ic200153n |*Inorg. Chem.* 2011, 50, 4195–4211

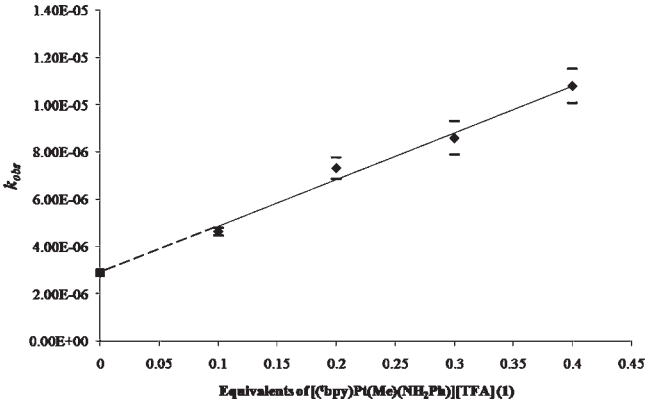

Figure 10. Plot of k_{obs} versus equivalents of complex **1** for conversion of complex **2** and phenylacetylene to aniline and complex **11** (R^2 = 0.98).

Scheme 1. Possible Reaction Pathway for Conversion of (^{t}bpy)Pt(Me)(NHPh) (2) and Phenylacetylene to (^{t}bpy)Pt(Me)(CCPh) (11) and Aniline Catalyzed by Impurity Complex 1

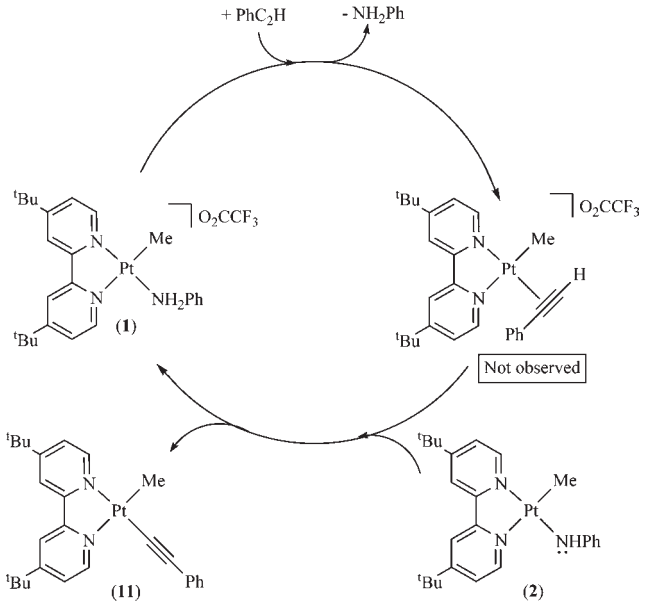

of formation of (^{t}bpy)Pt(Me)(C≡CPh) (**11**) (Figure 10). The reaction rate is first order in **1**. In principle, extrapolation of the linear regression for this plot to the *y* intercept should provide the intrinsic rate of the reaction of complex **2** and phenylacetylene in the absence of complex **1**. However, the deviation in the *y* intercept is too large to draw a reasonable conclusion about the intrinsic rate.

These results are consistent with trace amounts of the Pt−amine complex **1** catalyzing the conversion of the anilido complex **2** and phenylacetylene to the phenylacetylide complex **11** and aniline. Scheme 1 shows a possible reaction pathway that is catalytic in **1**. Starting with **1**, aniline/phenylacetylene ligand exchange would produce [(^{t}bpy)Pt(Me)(η^2-PhC≡CH)][TFA]. Deprotonation of [(^{t}bpy)Pt(Me)(η^2-PhC≡CH)][TFA] by (^{t}bpy)Pt(Me)(NHPh) (**2**) would produce complex **11** and reform the putative catalyst [(^{t}bpy)Pt(Me)(NH$_2$Ph)][TFA] (**1**). Alternatively, [(^{t}bpy)Pt(Me)(η^2-PhC≡CH)][TFA] could rearrange to a vinylidene complex, [(^{t}bpy)Pt(Me)(=C=CPhH)][TFA],[59] prior to deprotonation. No intermediates are observed by ^{1}H NMR spectroscopy for the conversion of complex **2** and phenylacetylene to complex **11**. Similar results were reported by our group for the conversion of TpRu(L)$_2$(NHPh) {L = PMe$_3$ or P(OMe)$_3$} and phenylacetylene to TpRu(L)$_2$(C≡CPh) and aniline.[53] Kinetic results were consistent with the TpRu(PMe$_3$)$_2$(OTf) complex, a precursor to TpRu(PMe$_3$)$_2$(NHPh), catalyzing the conversion of the anilido complex to TpRu(PMe$_3$)$_2$(C≡CPh). A similar mechanism to that in Scheme 1 was proposed to proceed through a Ru−vinylidene intermediate. In this case, the Ru−vinylidene complex was identified in the reaction mixture.[53] In addition, for the reaction of TpRu(PMe$_3$)$_2$NHPh and phenylacetylene, the formation of the Fischer carbene Tp(PMe$_3$)$_2$Ru=C(CH$_2$Ph)(NHPh), presumably from reaction of aniline and the Ru−vinylidene complex, is observed. An analogous carbene complex {i.e., [(^{t}bpy)(Me)Pt=C(CH$_2$Ph)(NHPh)]$^+$} is not observed in the Pt-based reaction.

Our group and others have reported the activation of R−H (R = aryl or H) bonds with late transition metal hydroxide and amido complexes via net 1,2-addition of R−H across the metal−heteroatom bond.[12−16,22,24,49,50,60] From a coordinated hydrocarbon species, it has been suggested that the presence of the basic lone pair on the heteroatomic ligand might provide an inherent kinetic advantage to C−H activation compared to a metal−alkyl complex; however, there are no reports of C−H activation with a metal center bearing both an alkyl and a heteroatomic ligand to provide a direct comparison.[12,22,50] The synthesis of complex **2** provides a system with both an alkyl and a heteroatomic ligand and could provide an internal competition for C−H activation and allow a direct comparison of C−H activation rates (i.e., C−H activation across the Pt−NHPh bond versus the Pt−CH$_3$ bond). However, previously reported Pt(II) systems that perform C−H activation typically require the generation of a three-coordinate reactive species.[61−63] Thus, we considered that the coordination of a C−H bond by complex **2** and C−H activation was not likely and chose to study H$_2$ activation as a model. We anticipated that the reaction of complex **2** with H$_2$ could result in coordination of dihydrogen to form a five-coordinate intermediate, H−H activation across the methyl or anilido ligands, methane or amine dissociation, and formation of the corresponding Pt−hydride complexes (Scheme 2).

The reaction of complex **2** with H$_2$ (room temperature) produces free ^{t}bpy ligand, CH$_4$, and aniline after approximately 12 h. At 45 psi of H$_2$, the formation of an intermediate complex, (^{t}bpy)Pt(Me)(H), is observed by ^{1}H NMR spectroscopy after 7 h (Scheme 3). For (^{t}bpy)Pt(Me)(H), a hydride resonance is observed at −14.8 ppm in the ^{1}H NMR spectrum (singlet with Pt satellites, $^1J_{Pt-H}$ = 1575 Hz) as well as a new methyl resonance at 2.21 ppm (singlet with Pt satellites, $^2J_{Pt-H}$ = 83 Hz). Our group and others have previously reported the 1,2-addition of H$_2$ across metal−heteroatom bonds.[64−69] For example, the five-coordinate (PCP)Ru(CO)(NH$_2$) [PCP = 2,6-(CH$_2$P^{t}Bu$_2$)$_2$C$_6$H$_3$] complex reacts with H$_2$ at room temperature to give (PCP)Ru(CO)(H) and ammonia.[68] Mechanistic studies suggest a pathway that involves coordination of H$_2$, 1,2-addition across the Ru−amido bond to yield (PCP)Ru(CO)(H)(NH$_3$), and ammonia dissociation. Fryzuk et al. reported a similar 1,2-H,H addition reaction with a Ru(II) complex

Scheme 2. Possible Reaction Pathways for Reaction of Complex 2 with Dihydrogen

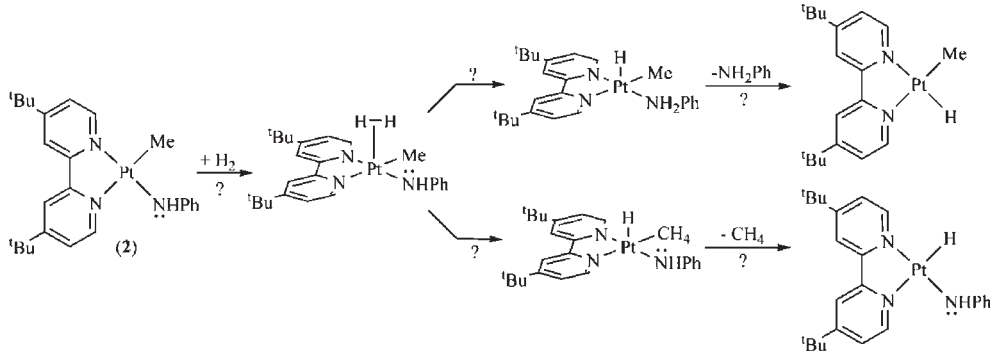

bearing a chelating amido ligand.[66] Morris et al. demonstrated that the reaction of H_2 with a Ru(II) amido complex produces a dihydrogen complex in which the H−H bond is intermediate between dihydrogen and protic-hydridic bonding.[70] Goldberg, Kemp, et al. reported the activation of dihydrogen across Pd(II)−OR (R = H or CH_3) complexes via a σ-bond metathesis-type transition state to produce ROH and a Pd(II)−H complex.[67] Thus, reaction of H_2 with **2** via a similar mechanism would involve coordination of H_2 to give (^{t}bpy)Pt(Me)(NHPh)(η^2-H_2), followed by 1,2-H,H addition to give (^{t}bpy)Pt(Me)(NH_2Ph)(H), and aniline dissociation to form free NH_2Ph and (^{t}bpy)Pt(Me)(H). Free ^{t}bpy, methane, and Pt(s) would then be formed by subsequent decomposition. However, after monitoring multiple reactions (^{1}H NMR spectroscopy) of the same concentration of **2** with H_2 at room temperature over a period of 8 h, plots of [**2**] versus time reveal inconsistent induction periods (Figure 11, plot A) as well as varied rates (Table 4). The observation of an induction period led us to consider that Pt(s) is serving as a heterogeneous catalyst.[71]

As an initial probe, a standard Hg test was used to suppress reactivity from in situ Pt(s) formation.[71] Elemental mercury was added to a solution of **2** in C_6D_6 followed by pressurization with H_2. The reaction was monitored (^{1}H NMR spectroscopy) over 7 h. The addition of elemental mercury results in complete suppression of reactivity (Figure 11, plot B). Next, a solution of **2** pressurized with H_2 was allowed to react until conversion of **2** and visible Pt(s) formation was observed. The reaction solution was then decanted to leave the solid, and a fresh solution of **2** in C_6D_6 was added to the original NMR tube, pressurized with H_2. For this fresh solution with "generated" Pt(s), a plot of [**2**] versus time revealed a line for the conversion of **2** and H_2 without an induction period, indicative of a reaction with a zero-order dependence on complex **2** (Figure 11, plot C). Maitlis' test[72] was performed by monitoring the reaction through the induction period and the beginning of the reaction. The reaction tube was then vented, the solution filtered through Celite, and the filtrate placed in a clean NMR tube, pressurized with H_2, and monitored (^{1}H NMR spectroscopy) for ~2 h. Figure 11 (plot D) shows that after removal of the Pt(s), there is a second induction period. As additional confirmation, 10 wt % Pt on activated carbon was added to a solution of **2** before pressurization with H_2. Following the addition of H_2, the reaction reached 50% conversion after 5 min and reached completion in less than 1 h.

For hydrogenolysis of (PCP)Pd(OH), Goldberg, Kemp et al. reported a mechanism that involves coordination of H_2 followed

Scheme 3. Proposed Reaction Sequence for Reaction of Complex 2 with Dihydrogen

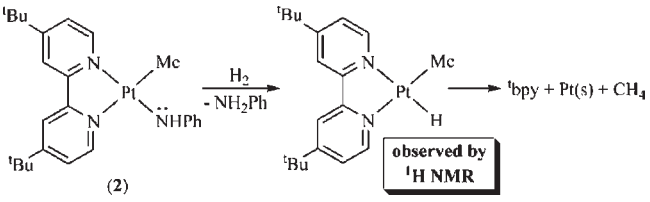

by an intramolecular proton transfer through a four-centered transition state. The proposed pathway of H_2 addition across the Pt−NHPh bond of complex **2** is different than the proposed mechanism for the Pd(II) hydroxide and methoxide complexes reported by Goldberg, Kemp et al.[67] To probe the source of these differences, we employed DFT calculations (B3LYP, double-ζ-plus-polarization pseudopotential basis sets) using 2,2′-bipyridine (bpy) as a model for the ^{t}bpy ligand. The overall reaction of (bpy)Pt(Me)(NHPh) (**2′**) and H_2 to give (bpy)Pt(Me)(H) and free aniline is calculated to be exothermic by 6 kcal/mol. However, this reaction is calculated to occur with an enthalpy of activation of 45 kcal/mol (Scheme 4). In contrast, the previously calculated enthalpy of activation barrier for H_2 addition across the Pd−OH bond of (PCP′)Pd(OH) {PCP′ = 2,6-bis-$(CH_2PMe_2)_2C_6H_3$} to give (PCP′)Pd(H) and water is 21.0 kcal/mol, despite the similar overall reaction enthalpy (−4 kcal/mol).[67] The calculated reaction enthalpy and H_2 activation barrier for the corresponding Pd−methoxide complex (PCP′)Pd(OMe) are similar to those of the hydroxyl analogue (−3 and 24 kcal/mol, respectively).[67]

Although the calculations reveal a substantial difference in the activation barrier for H−H bond cleavage by the (PCP′)Pd(OH)/(OMe) and (^{t}bpy)Pt(Me)(NHPh) systems, the source of the difference is not obvious. In order to probe these differences, we performed calculations by varying the ligand X, metal, and ancillary ligand (PCP versus bpy). Systematic changes reveal an impact on the enthalpy of activation by ~5−10 kcal/mol for each alteration. Scheme 5 provides an overview of the calculations for each variation, and Figure 12 provides key bond distances for all of the calculated transition states. No correlations that would lead us to confidently invoke trends based on early versus late transition states could be found among the calculated transition state metrics and the activation barriers (or calculated enthalpies).

dx.doi.org/10.1021/ic200153n |*Inorg. Chem.* 2011, 50, 4195–4211

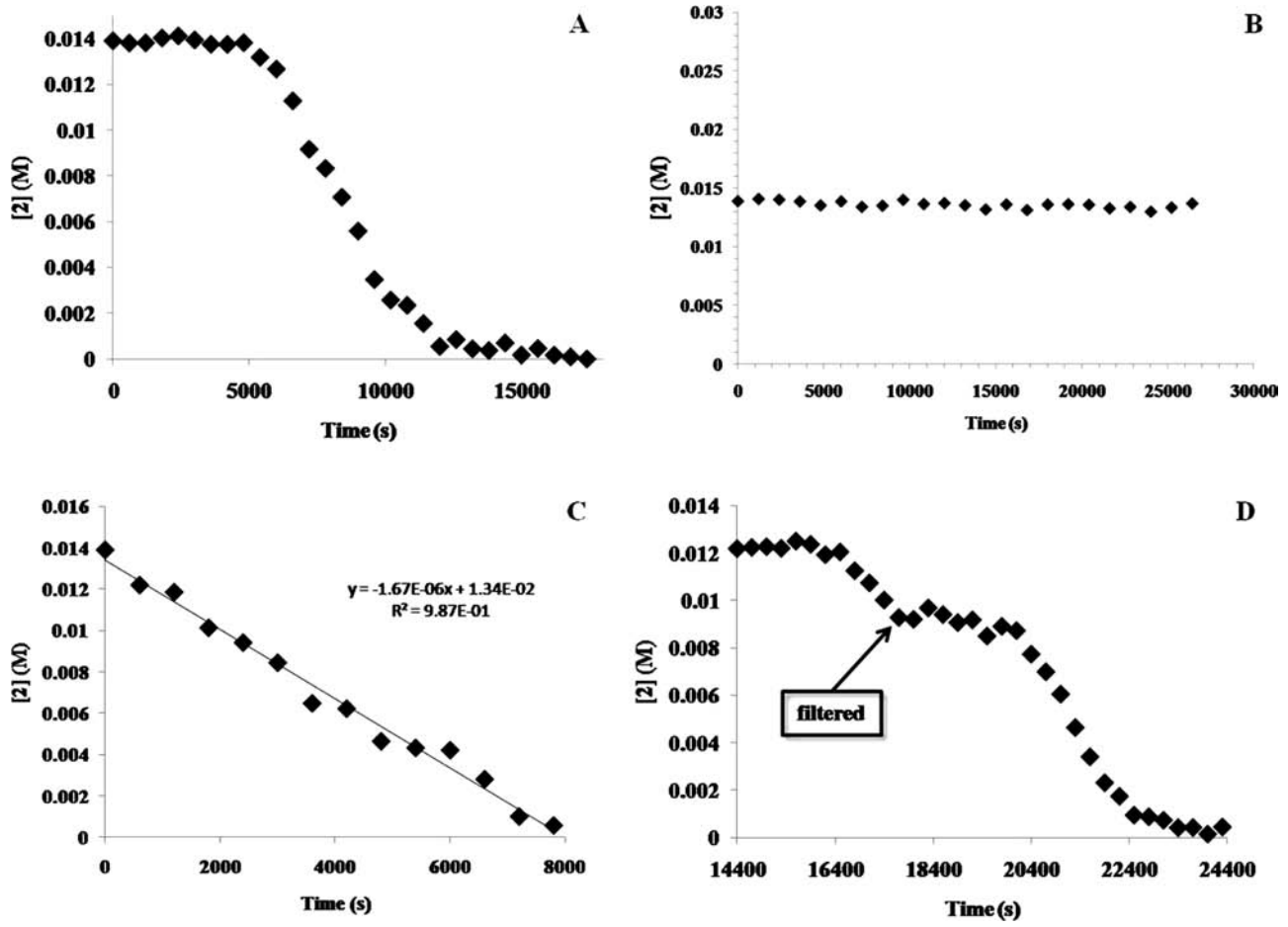

Figure 11. Plots monitoring [**2**] versus time for conversion of **2** and H_2 to free ^{t}bpy, aniline, methane, and Pt(s): (A) 200 psi of H_2 at room temperature, (B) elemental Hg added at the beginning of reaction, (C) fresh solution of **2** added to a tube with "generated" Pt(s), and (D) reaction solution filtered to remove Pt(s) after initial induction period (plot started after 14 400 s reaction time).

Table 4. Summary of Experimental Trials for Reaction of Complex 2 and H_2

experiment	induction period (s)	rate[a] (s^{-1})
1	4800	2.0×10^{-6}
2	6000	2.6×10^{-6}
3	9600	3.0×10^{-6}
4	4200	2.2×10^{-6}

[a] Rate after the induction period.

Scheme 4. Calculated Reaction Enthalpy (DFT, B3LYP) and Enthalpy of Activation for Reaction of Complex 2′ with H_2

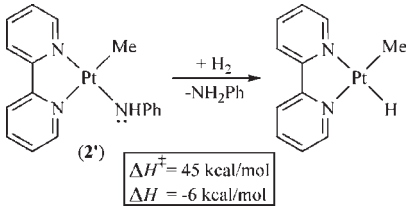

One major difference between (PCP′)Pd(OH) and (bpy)Pt(Me)(NHPh) may be the affinity for H_2 coordination and, hence, activation of H_2. Consistent with this suggestion, our calculations reveal that H_2 does not form a stable bond with complex **2**. Attempts to isolate a bound H_2 adduct of complex **2** were not successful. Geometry optimizations converged to stationary points in which H_2 and complex **2** are well separated. This is potentially explained by the anticipated decrease in electrophilicity of Pt relative to Pd. When the metal center of (bpy)Pt(Me)(NHPh) is substituted with Pd to give (bpy)Pd(Me)(NHPh), although the overall ΔH becomes less favorable by 2.6 kcal/mol, there is a decrease in the enthalpy of activation of 7.4 kcal/mol. Variation of the ligand X and ancillary ligand also impacts the activation barrier significantly. For example, replacing the anilido ligand in (bpy)Pt(Me)(NHPh) with NHMe or OMe decreases the activation barrier from 45.5 to 37.4 or 40.1 kcal/mol. The calculated activation barrier from (bpy)Pd(Me)(OMe) is 33.2 kcal/mol, and substitution of bpy and the methyl ligand with PCP′ to give (PCP′)Pd(OMe) lowers the barrier by 9.2 to 24.0 kcal/mol.

In addition to metal electrophilicity, steric and electronic contributions from the heteroatomic ligand play a crucial role in the elevated barriers. Figure 13 displays the calculated transition state for H−H activation by complex **2**. In order for the amido lone pair to orient to receive H^+ from a coordinated H_2, which is positioned approximately above the Pt square plane

dx.doi.org/10.1021/ic200153n |*Inorg. Chem.* 2011, 50, 4195–4211

Scheme 5. Overview of Calculations (enthalpies in kcal/mol for the activation barrier and overall transformation) with Systematic Variation of the Ligand X, Metal, and Ancillary Ligand (bpy versus PCP) for Reaction of the Metal−Heteroatom Complexes with H_2[a]

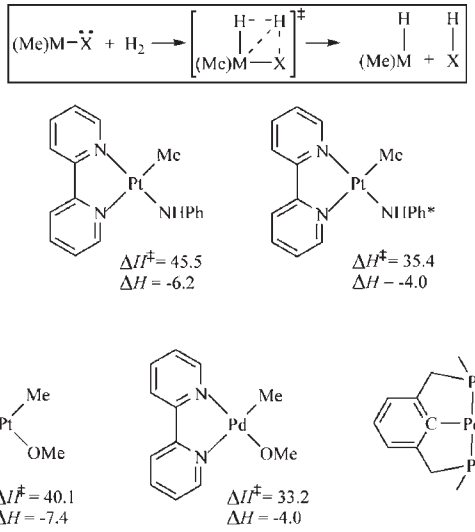

[a] Ph* = phenyl group modeled by the universal force field, enthalpies at 1 atm, 298.15 K.

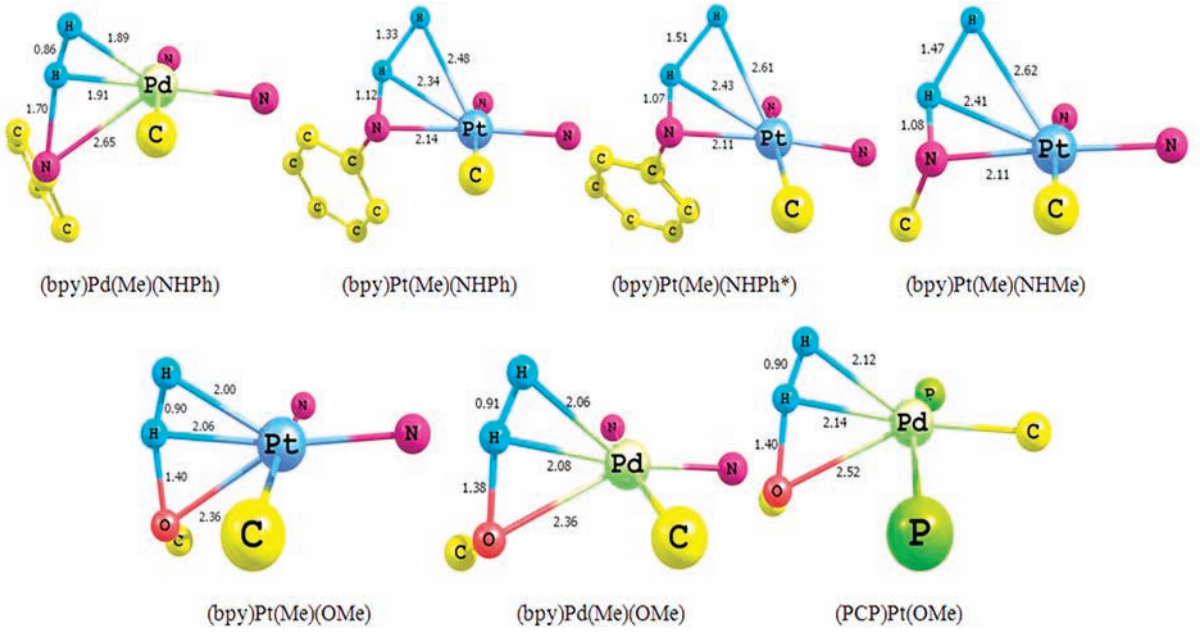

Figure 12. Overview of calculated transition state active sites (bond lengths in Angstroms) with systematic variation of metal (Pt vs Pd), activating ligand (NMe vs OMe vs NPh vs NPh*), and ancillary ligand (bpy vs PCP) for reaction of the metal−heteroatom complexes in Scheme 5 with H_2.

in the apical position, the amido lone pair must be aligned approximately perpendicular to the Pt square plane. This orientation places the phenyl group in close proximity to either the Me ligand or the ^{t}bpy ligand, which provides a steric inhibition to H_2 activation. In addition, the solid-state structure suggests that the amido lone pair is aligned for donation into the phenyl π^* system (Figure 2). However, for the lone pair to align perpendicular to the Pt square plane, the phenyl substituent must rotate perpendicular to the amide plane, breaking C_{ipso}−N conjugation. The calculated transition state reveals longer bond lengths of 1.46 Å for the C_{ipso}−N bond versus 1.39 Å (calculated, 1.36 Å experimental) in complex **2**. Thus, stabilization of the anilido lone pair into the phenyl π^* system is negated, resulting in an electronic inhibition to H_2 activation. These results may indicate the critical role that the lone pair on the −NHR and −OR ligands plays in the activation of H−H and C−H bonds.[12,22,50,60] For some of the calculated transition states, the bond distance between Pt and the incipient Pt−H is longer (>2.4 Å) than is expected for a 1,2-addition; however, for these complexes there is no evidence of an H_2 adduct that would precede the addition reaction. We believe that the unexpectedly long Pt−H bond distances are a result of this facet of the reaction, which perhaps

dx.doi.org/10.1021/ic200153n |*Inorg. Chem.* 2011, 50, 4195–4211

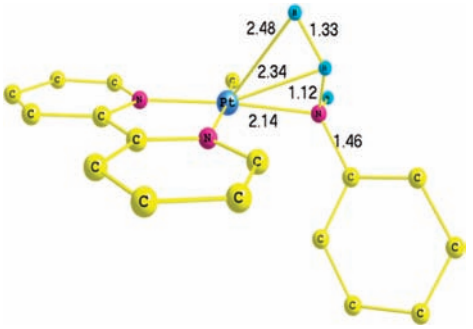

Figure 13. Calculated transition state for activation of H_2 by complex **2**. Most H atoms omitted for clarity.

closely resembles deprotonation of "free" dihydrogen and, hence, the substantial activation barriers.

Three-coordinate Pt(II) systems are known to activate C−H bonds.[61−63] Recently, our group reported the catalytic activation of aromatic C−H bonds with $[(^t\text{bpy})\text{Pt}(\text{Ph})(\text{L})][\text{BAr}'_4]$ [L = labile ligand; Ar′ = 3,5-$(\text{CF}_3)_2\text{C}_6\text{H}_3$].[73] To test the viability of performing C−H activation with analogous heteroatomic systems, complexes of the type $[(^t\text{bpy})\text{Pt}(\text{X})(\text{L})]^+$ (X = NHPh, OPh; L = pyridine, THF, NC_5F_5) were targeted.

When complex **4** is reacted with 1 equiv of HBAr'_4 in the presence of pyridine, the production of free aniline and $[(^t\text{bpy})\text{Pt}(\text{NHPh})(\text{py})][\text{BAr}'_4]$ (py = pyridine) (**12**) is observed (eq 12). Conversion from the neutral complex **4** to cationic **12** results in an upfield shift of the N*H* resonance from 3.8 (C_6D_6) to 2.90 ppm (CD_2Cl_2) in the ^{1}H NMR spectrum. The corresponding cationic phenoxide complex $[(^t\text{bpy})\text{Pt}(\text{OPh})(\text{py})][\text{BAr}'_4]$ (**13**) was prepared in a similar fashion (eq 13).

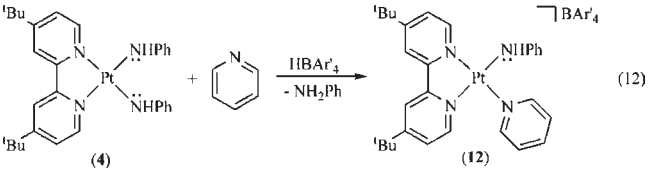

(12)

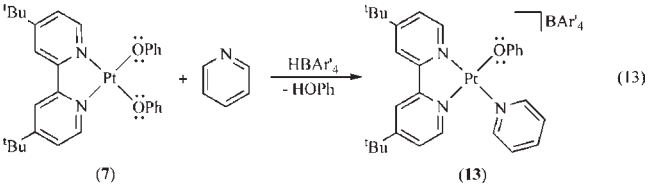

(13)

Complexes **12** and **13** were heated in C_6D_6 (100 °C) and monitored for the production of aniline and phenol, respectively. After heating for 72 h, aniline or phenol production was not observed. Careful monitoring of the N*H* resonance (2.90 ppm) of **12** also revealed no H/D exchange. To test the thermodynamic accessibility of the C−H activation reaction, the reverse reaction was attempted. Heating (24 h, 100 °C) $[(^t\text{bpy})\text{Pt}(\text{Ph})(\text{NC}_5\text{F}_5)][\text{BAr}'_4]$ and 1 equiv of pyridine with either aniline or phenol in dichloromethane-d_2 results in conversion to **12** or **13**, respectively (Scheme 6). These results indicate that the benzene C−H activation reactions are not thermodynamically favorable, but kinetic access to H/D exchange into the N*H* of complex **12** was still a possibility. For example, although direct C−H activation with $\text{TpRu}(\text{PMe}_3)_2(\text{X})$ (X = OH, NHPh) was not accessible, H/D exchange was observed into the hydroxide and anilido-N*H* ligands.[12,13]

It is possible that C−D activation of C_6D_6 was not observed for complex **12** because pyridine is bound too tightly to the metal center. Abstraction of the chloride ligand from complex **5** with AgBAr'_4 in the presence of more weakly coordinating solvents (e.g., THF or pentafluoropyridine) or a noncoordinating solvent results in the formation of the dimer $[(^t\text{bpy})\text{Pt}(\mu\text{-NHPh})]_2[\text{BAr}'_4]_2$ (**14**) (eq 14). Complex **14** exhibits three aryl ^{t}bpy resonances and one ^{t}Bu ^{t}bpy resonance integrating for 36 protons. Heating complex **14** in benzene (C_6D_6, 120 °C) results in no change in the ^{1}H NMR spectrum.

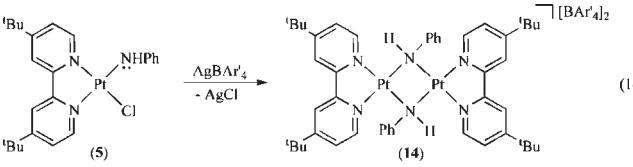

(14)

SUMMARY AND CONCLUSIONS

Herein, we report the preparation of neutral and cationic Pt(II) anilido and phenoxide systems and studied their reactions with H_2 and substrates that possess C−H bonds. Salient points include:

(1) The 1,2-addition of C−H and H−H bonds across Pt(II)−X bonds is not accessible from four-coordinate $(^t\text{bpy})\text{Pt}(\text{X})(\text{Y})$ or $[(^t\text{bpy})\text{Pt}(\text{X})(\text{L})]^+$ systems. For the activation of H_2 by $(^t\text{bpy})\text{Pt}(\text{Me})(\text{NHPh})$, which we studied computationally and experimentally, several aspects appear to preclude access to the 1,2-addition reaction via initial H_2 coordination to give five-coordinate $(^t\text{bpy})\text{Pt}(\text{Me})(\text{NHPh})(\text{H}_2)$ followed by H−H addition across the Pt−NHPh bond to give $(^t\text{bpy})\text{Pt}(\text{Me})(\text{NH}_2\text{Ph})(\text{H})$. Our studies suggest the factors that contribute to the substantial activation barrier (calculated $\Delta H^{\ddagger}$ = 45 kcal/mol) include ancillary ligand identity, decreased Pt electrophilicity (compared, for example, to a related Pd system), and steric constraints. For example, in order for the amido lone pair to orient perpendicular to the square plane to receive H^+ from coordinated H_2, the phenyl group is placed in close proximity to either the methyl or ^{t}bpy ligand, providing a steric inhibition to H_2 activation. In addition, the DFT calculations suggest that simple coordination of H_2 to $(^t\text{bpy})\text{Pt}(\text{Me})(\text{NHPh})$ is not favorable, and the strongly donating anilido and methyl ligands likely play a role here.

(2) Four-coordinate $(^t\text{bpy})\text{Pt}(\text{X})(\text{Y})$ complexes can provide net activation of acidic C−H bonds (e.g., phenylacetylene); however, the reaction is catalyzed by an impurity and likely does not proceed by a 1,2-CH-addition pathway. Thus, even for "activated" C−H bonds, the 1,2-CH-addition process via a five-coordinate intermediate does not appear to be facile.

(3) Elemental platinum serves as a catalyst for the 1,2-addition of H_2 across a Pt−NHPh bond. To our knowledge, this is the first report of a heterogeneous catalyst activating covalent bonds toward addition across a metal−heteroatom bond and provides a caveat to

dx.doi.org/10.1021/ic200153n |*Inorg. Chem.* 2011, 50, 4195–4211

Scheme 6. Reaction of $[(^t\text{bpy})\text{Pt}(\text{Ph})(\text{NC}_5\text{F}_5)][\text{BAr}'_4]$ with Aniline and Phenol to Form Complexes 12 and 13

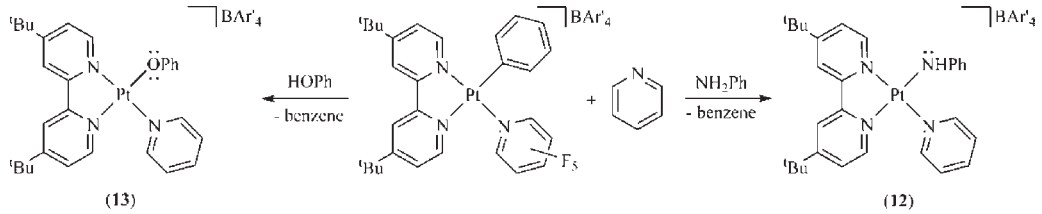

mechanistic conclusions for related reactions in the absence of kinetic data.[74,75]

(4) Similar to C−H activation by related Pt(II) systems with hydrocarbyl or halide ligands,[61−63,76,77] the 1,2-addition of C−H bonds from 3-coordinate $[(^t\text{bpy})\text{Pt(X)}]^+$ complexes could be feasible. However, $[(^t\text{bpy})\text{Pt(X)(py)}]^+$ complexes did not activate C−H bonds, perhaps because pyridine is too tightly bound. For the anilido complex, attempts to replace pyridine with less strongly donating ligands resulted in the formation of a μ-NHPh binuclear complex. This system did not activate C−H bonds, which is likely due to the inability to access the desired 3-coordinate Pt(II) cations.

These results suggest that the key factor for observing 1,2-CH-addition across M−X bonds of d^8 systems is access to coordinatively unsaturated systems (i.e., 3-coordinate). Given the ability of "X" ligands (e.g., OR, NHR) to bridge electrophilic metals, this will likely require a subtle steric balance that promotes coordinative unsaturation but does not inhibit hydrocarbon coordination.

EXPERIMENTAL SECTION

General Methods. All procedures were performed under anaerobic conditions in a nitrogen-filled glovebox or using standard Schlenk techniques. Glovebox purity was maintained by periodic nitrogen purges and monitored by an oxygen analyzer (O_2 < 15 ppm for all reactions). Benzene, toluene, and tetrahydrofuran were purified by distillation over sodium/benzophenone. Pentane was distilled over P_2O_5 prior to use. Diethyl ether and pyridine were distilled over CaH_2 prior to use. Hexanes and methylene chloride were purified by passage through a column of activated alumina. Benzene-d_6, chloroform-d_1, acetone-d_6, and methylene chloride-d_2 were degassed via three freeze−pump−thaw cycles and stored under nitrogen atmosphere over 4 Å molecular sieves. Tetrahydrofuran-d_8 was used as received in glass ampules packed under dinitrogen. Aniline was dried over CaH_2, vacuum distilled, and stored under a nitrogen atmosphere over 4 Å molecular sieves. All other reagents were used as purchased from commercial sources. ^{1}H and ^{13}C NMR spectra were acquired using Varian Mercury spectrometers operating at 300 (^{1}H NMR) and 75 MHz (^{13}C NMR) and are referenced to tetramethylsilane using residual proton signals or the ^{13}C resonances of the deuterated solvent. ^{19}F NMR spectra were acquired using a Varian Mercury spectrometer operating at 282 MHz with C_6F_6 (−163.0 ppm) as the external standard. All NMR spectra were acquired at room temperature unless otherwise noted. Thick-walled high-pressure glass NMR tubes with a PV-ANV Teflon valve (maximum pressure rating 200 psi) were purchased from Wilmad-Labglass and used for all 200 psi H_2 experiments. Tubes were charged with H_2 using a stainless steel gas pressure line (maximum pressure rating 3000 psi) connected directly to the gas cylinder. Elemental analyses were performed by Atlantic Microlabs, Inc. Synthetic and characterization details of $NaBAr'_4$,[78] $HBAr'_4$,[79] $AgBAr'_4$,[80] $(^t\text{bpy})\text{Pt(Me)}_2$,[31] $(^t\text{bpy})\text{Pt(Me)(TFA)}$,[25] $(^t\text{bpy})\text{Pt(OTf)}_2$,[25] and $(^t\text{bpy})\text{Pt(Ph)}_2$[81] have been previously reported. Phenylacetylene was passed through a column of activated alumina prior to use.

$[(^t\text{bpy})\text{Pt(Me)(NH}_2\text{Ph)}][\text{TFA}]$ (1). $(^t\text{bpy})\text{Pt(Me)(TFA)}$ (0.058 g, 0.099 mmol) (TFA = O_2CCF_3) was dissolved in toluene (5 mL) in a pressure tube. After addition of aniline (0.027 mL, 0.30 mmol), the tube was sealed and heated to 90 °C for 24 h. After removal of volatiles in vacuo, the resulting residue was reconstituted in THF and filtered through Celite. The filtrate was reduced in vacuo to a residue. After dissolution in methylene chloride (∼ 1 mL), the addition of hexanes resulted in the formation of a yellow precipitate, which was collected and dried in vacuo (0.056 g, 83% yield). ^{1}H NMR (C_6D_6, δ): 9.42 (d, 1H, $^3J_{\text{H5−H6}}$ = 6 Hz, ^{t}bpy 6/6′), 8.45, 8.30 (each a d, each 1H, $^4J_{\text{H3−H5}}$ = 2 Hz, ^{t}bpy 3/3′), 8.26 (d, 1H, $^3J_{\text{H5−H6}}$ = 6 Hz, ^{t}bpy 6/6′), 7.88 (d, 2H, $^3J_{\text{HH}}$ = 7 Hz, aniline-*ortho*), 7.72 (br s, 2H, Pt−NH_2Ph), 7.04−6.98 (m, 3H, overlap of aniline-*meta* and ^{t}bpy 5/5′), 6.80 (t, 1H, $^3J_{\text{HH}}$ = 7 Hz, aniline-*para*), 6.67 (dd, 1H, $^3J_{\text{H5−H6}}$ = 6 Hz, $^4J_{\text{H3−H5}}$ = 2 Hz, ^{t}bpy 5/5′), 1.19, 1.06 (each a s, each 9H, ^{t}bpy ^{t}Bu), 0.84 (s with Pt satellites, 3H, $^2J_{\text{Pt−H}}$ = 70 Hz, Pt−CH_3). ^{13}C{^{1}H} NMR (CD_2Cl_2, δ): 164.6, 164.2, 150.3, 149.2, 142.8, 129.7, 126.5, 125.9, 124.7, 124.1, 120.4, 119.7, 118.6, 115.3 (each a s, ^{t}bpy aromatic and anilido-phenyl carbons), 36.3 {s, ^{t}Bu-$C(CH_3)_3$, one signal missing presumably due to coincidental overlap}, 30.5, 30.4 {each a s, ^{t}Bu-C$(CH_3)_3$}, −10.4 (singlet with Pt satellites, $^1J_{\text{Pt−C}}$ = 774 Hz, Pt-CH_3); Note: carbons of O_2CCF_3 were not located. ^{19}F NMR (C_6D_6, δ): −74.5 (s, O_2CCF_3). Anal. Calcd for $C_{27}H_{34}F_3N_3O_2Pt$: C, 47.37; H, 5.01; N, 6.14. Found: C, 46.82; H, 4.94; N, 5.97.

$(^t\text{bpy})\text{Pt(Me)(NHPh)}$ (2). In a round-bottom flask, a yellow homogeneous solution of $[(^t\text{bpy})\text{Pt(Me)(NH}_2\text{Ph)}][\text{TFA}]$ (**1**) (0.045 g, 0.066 mmol) in ∼15 mL of benzene was prepared. Upon addition of a THF solution of $Na[N(SiMe_3)_2]$ (0.066 mL, 0.066 mmol), a color change to deep green was observed. The resulting mixture was stirred for 2 h and then filtered through Celite. The filtrate was reduced in vacuo to a green solid (0.032 g, 85% yield). A crystal suitable for an X-ray diffraction study was grown by slow evaporation of a diethyl ether solution of **2**. ^{1}H NMR (C_6D_6, δ): 9.37, 8.97 (each a d, each 1H, $^3J_{\text{H5−H6}}$ = 6 Hz, ^{t}bpy 6/6′), 7.40−7.28 (m, 6H, overlap of ^{t}bpy 3/3′ with anilido-*ortho* and −*meta*), 6.65 (tt, 1H, $^4J_{\text{HH}}$ = 7 Hz, $^3J_{\text{HH}}$ = 2 Hz, anilido-*para*), 6.46, 6.42 (each a dd, each 1H, $^3J_{\text{H5−H6}}$ = 6 Hz, $^4J_{\text{H3−H5}}$ = 2 Hz, ^{t}bpy 5/5′), 3.99 (br s, 1H, Pt−N*H*Ph), 1.85 (s with Pt satellites, 3H, $^2J_{\text{Pt−H}}$ = 84 Hz, Pt−CH_3), 0.95, 0.89 (each a s, each 9H, ^{t}bpy ^{t}Bu). ^{13}C{^{1}H} NMR (acetone-d_6, δ): 163.2, 162.6, 149.2, 148.9, 129.2, 128.9, 125.2, 124.8, 121.8, 120.6, 116.7, 110.3 (each a s, ^{t}bpy and NH-phenyl carbons, two signals missing presumably due to coincidental overlap), 36.5 (s, ^{t}Bu-$C(CH_3)_3$, one signal missing presumably due to coincidental overlap), 30.5, 30.3 (each a s, ^{t}BuC$(CH_3)_3$), −14.2 (singlet with Pt satellites, $^1J_{\text{Pt−C}}$ = 813 Hz, Pt-CH_3). Anal. Calcd for $C_{25}H_{33}N_3Pt$: C, 52.62; H, 5.83; N, 7.36. Found: C, 53.31; H, 5.88; N, 7.37.

$[(^t\text{bpy})\text{Pt(NH}_2\text{Ph)}_2][\text{OTf}]_2$ (3). A homogeneous solution of $(^t\text{bpy})\text{Pt(OTf)}_2$ (0.042 g, 0.056 mmol) in methylene chloride (5 mL) was prepared. Upon addition of aniline (0.020 mL, 0.22 mmol) an

dx.doi.org/10.1021/ic200153n |*Inorg. Chem.* 2011, 50, 4195–4211

immediate color change from yellow to green was observed. After stirring for 30 min, the volatiles were removed in vacuo. Reconstitution in THF followed by addition of hexanes resulted in the precipitation of a green solid. The solid was collected by filtration through a fine-porosity frit and washed with hexanes (2 × 5 mL) and diethyl ether (2 × 5 mL) (0.041 g, 78% yield). A crystal suitable for an X-ray diffraction study was grown by slow diffusion of a THF solution of **3** layered with hexanes. ^{1}H NMR ($CDCl_3$, δ): 8.50 (d, 2H, $^3J_{H5-H6}$ = 6 Hz, ^{t}bpy 6/6′), 7.92 (d, 2H, $^4J_{H3-H5}$ = 2 Hz, ^{t}bpy 3/3′), 7.69 (d, 4H, $^3J_{HH}$ = 8 Hz, aniline-*ortho*), 7.65 (br s, 4H, aniline N*H*$_2$), 7.54 (dd, 2H, $^3J_{H5-H6}$ = 6 Hz, $^4J_{H3-H5}$ = 2 Hz, ^{t}bpy 5/5′), 7.25−7.22 (m, 6H, overlap of aniline-*meta* and -*para*), 1.40 (s, 18H, ^{t}bpy ^{t}Bu). ^{13}C{^{1}H} NMR ($CDCl_3$, δ): 167.1, 156.2, 150.5, 138.6, 130.1, 128.1, 125.6, 124.7, 120.5 (each a s, ^{t}bpy and NH-phenyl carbons), 120.4 (q, $^1J_{C-F}$ = 318 Hz, O_3SCF_3), 36.3 (s, ^{t}Bu *C*(CH$_3$)$_3$), 30.2 (s, ^{t}Bu C(*C*H$_3$)$_3$). ^{19}F NMR (282.2 MHz, $CDCl_3$, δ): −78.6 (s, O_3SCF_3). Anal. Calcd for $C_{32}H_{38}F_6N_4O_6PtS_2$: C, 40.55; H, 4.04; N, 5.91. Found: C, 40.82; H, 3.97; N, 5.88.

(^{t}bpy)Pt(NHPh)$_2$ (4). [(^{t}bpy)Pt(NH$_2$Ph)$_2$][OTf]$_2$ (**3**) (0.089 g, 0.093 mmol) was dissolved in benzene (5 mL) to give a green solution. Upon addition of Na[N(SiMe$_3$)$_2$] (0.19 mL, 0.19 mmol) a blue-green mixture was observed. After 2 h, the blue suspension was filtered through Celite and the filtrate was reduced to dryness. Reconstitution in minimal THF and addition of hexanes gave a fine blue precipitate, which was collected by filtration through a fine-porosity frit and washed with hexanes (2 × 10 mL) (0.020 g, 71% yield). A crystal suitable for an X-ray diffraction study was grown by slow diffusion of a methylene chloride solution of **4** layered with hexanes. ^{1}H NMR (C_6D_6, δ): 9.32 (d, 2H, $^3J_{H5-H6}$ = 6 Hz, ^{t}bpy 6/6′), 7.30−7.25 (m, 8H, overlap of anilido-*ortho* and -*meta*), 7.18−7.16 (m, 2H, overlap of solvent and ^{t}bpy 3/3′), 6.69−6.62 (m, 2H, anilido-*para*), 6.32 (dd, 2H, $^3J_{H5-H6}$ = 6 Hz, $^4J_{H3-H5}$ = 2 Hz, ^{t}bpy 5/5′), 3.80 (br s, 2H, Pt−N*H*Ph), 0.89 (s, 18H, ^{t}bpy ^{t}Bu). ^{13}C{^{1}H} NMR (THF-d_8, δ): 163.6, 160.1, 158.5, 151.5, 128.9, 124.8, 120.6, 116.9, 111.6 (each a s, ^{t}bpy aryl and NH-phenyl carbons), 36.7 (s, ^{t}Bu *C*(CH$_3$)$_3$), 30.4 (s, ^{t}Bu C(*C*H$_3$)$_3$). Anal. Calcd for $C_{30}H_{36}N_4Pt$: C, 55.63; H, 5.60; N, 8.65. Found: C, 55.76; H, 5.72; N, 8.42.

(^{t}bpy)Pt(NHPh)(Cl) (5). In a Schlenk flask, (^{t}bpy)Pt(NHPh)$_2$ (**4**) (0.032 g, 0.048 mmol) was prepared as a blue-green solution in benzene (5 mL). The addition of HCl (1.0 M diethyl ether solution, 0.048 mL, 0.048 mmol) resulted in a color change to deep green. After stirring for 1 h, the volatiles were reduced in vacuo to approximately 1 mL, and hexanes were added to give a blue solid. The solid was collected by filtration through a fine-porosity frit and washed with hexanes (2 × 10 mL) and diethyl ether (2 × 10 mL) (0.021 g, 75% yield). ^{1}H NMR (C_6D_6, δ): 9.53, 9.27 (each a d, each 1H, $^3J_{H5-H6}$ = 6 Hz, ^{t}bpy 6/6′), 7.39−7.21 (m, 6H, overlap of anilido-*ortho* and -*meta* and ^{t}bpy 3/3′), 6.68−6.62 (m, 2H, overlap of anilido-*para* and ^{t}bpy 5), 6.33 (dd, 1H, $^3J_{H5-H6}$ = 6 Hz, $^4J_{H3-H5}$ = 2 Hz, ^{t}bpy 5′), 4.06 (br s, 1H, Pt−N*H*Ph), 0.99, 0.91 (each an s, each 9H, ^{t}bpy ^{t}Bu). ^{13}C{^{1}H} NMR (THF-d_8, δ): 164.2, 163.9, 161.6, 159.9, 151.05, 150.2, 129.2, 128.8, 125.0, 124.9, 121.0, 120.8, 117.5, 112.4 (each a s, ^{t}bpy and NH-phenyl carbons), 36.8, 36.7 (each a s, ^{t}Bu-*C*(CH$_3$)$_3$), 30.5, 30.4 (each a s, ^{t}Bu-C(*C*H$_3$)$_3$). Anal. Calcd for $C_{24}H_{30}ClN_3Pt$: C, 48.77; H, 5.12; N, 7.11. Found: C, 48.48; H, 5.08; N, 6.98.

(^{t}bpy)Pt(Me)(OPh)·HOPh (6). (^{t}bpy)Pt(Me)$_2$ (0.10 g, 0.20 mmol) and phenol (0.186 g, 1.97 mmol) were combined in a round-bottom flask in benzene (∼20 mL). After stirring the red suspension for 2 h, the volatiles were reduced in vacuo to ∼1 mL. The addition of hexanes resulted in a yellow precipitate that was collected by filtration through a fine-porosity frit. The resulting solid was rinsed with pentane (2 × 3 mL) and diethyl ether (3 × 3 mL) (0.092 g, 82% yield). ^{1}H NMR (acetone-d_6, δ): 9.05, 8.77 (each a d, each 1H, $^3J_{H5-H6}$ = 6 Hz, ^{t}bpy 6/6′), 8.53, 8.47 (each a d, each 1H, $^4J_{H3-H5}$ = 2 Hz, ^{t}bpy 3/3′), 7.78, 7.63 (each a dd, each 1H, $^3J_{H5-H6}$ = 6 Hz, $^4J_{H3-H5}$ = 2 Hz, ^{t}bpy 5 and 5′), 7.17 (t, 1H, $^3J_{HH}$ = 8 Hz, phenoxy/phenol-*para*), 7.06−6.75 (m, 8H, overlap of phenoxy/phenol-*ortho* and -*meta*), 6.34 (t, 1H, $^3J_{HH}$ = 7 Hz, phenoxy/phenol-*para*), 3.79 (br s phenol-O*H*), 1.45, 1.43 (each a s, each 9H, ^{t}bpy ^{t}Bu), 1.00 (singlet with Pt satellites, $^2J_{Pt-H}$ = 82 Hz, Pt−C*H*$_3$). ^{13}C{^{1}H} NMR (acetone-d_6, δ): 171.1, 164.3, 163.4, 156.9, 155.6, 151.1, 147.6, 129.6, 128.5, 128.2, 124.7, 124.4, 121.4, 120.1, 119.8, 119.4, 115.5, 113.5 (each a s, ^{t}bpy, phenoxy, and 1 equiv of H-bonded phenol carbons), 36.6 (s, ^{t}Bu-*C*(CH$_3$)$_3$, one signal missing presumably due to coincidental overlap), 30.5, 30.2 {each a s, ^{t}Bu-C(*C*H$_3$)$_3$}, −14.2 (singlet with Pt satellites, $^1J_{Pt-C}$ = 826 Hz, Pt-*C*H$_3$). Anal. Calcd for $C_{25}H_{32}N_2OPt\cdot C_6H_6O$: C, 55.93; H, 5.75; N, 4.21. Found: C, 56.46; H, 5.78; N, 4.19. Note: 1 equiv of phenol confirmed by ^{1}H NMR.

(^{t}bpy)Pt(OPh)$_2$ (7). (^{t}bpy)Pt(NHPh)$_2$ (**4**) (0.140 g, 0.216 mmol) and THF (10 mL) were combined in a thick-walled glass pressure tube. After the addition of phenol (0.083 g, 0.88 mmol), the tube was sealed with a PTFE screw cap. The mixture was heated at 80 °C for ∼12 h in a temperature-controlled oil bath. After cooling to room temperature, the solvent was reduced in vacuo to ∼1 mL. The addition of hexanes resulted in the precipitation of a green solid. The solid was collected by filtration through a fine-porosity frit and washed with hot hexanes (5 × 2 mL) to remove excess phenol (0.134 g, 95% yield). A crystal suitable for an X-ray diffraction study was grown by slow diffusion of a THF solution layered with hexanes. ^{1}H NMR (acetone-d_6, δ): 8.88 (d, 2H, $^3J_{H5-H6}$ = 6 Hz, ^{t}bpy 6/6′), 8.55 (d, 2H, $^4J_{H3-H5}$ = 2 Hz, ^{t}bpy 3/3′), 7.80 (dd, 2H, $^3J_{H5-H6}$ = 6 Hz, $^4J_{H3-H5}$ = 2 Hz, ^{t}bpy 5/5′), 7.15 (d, 4H, $^3J_{HH}$ = 8 Hz, phenoxy-*ortho*), 6.89 (t, 4H, $^3J_{HH}$ = 8 Hz, phenoxy-*meta*), 6.36 (t, 2H, $^3J_{HH}$ = 8 Hz, phenoxy-*para*), 1.44 (s, 18H, ^{t}bpy ^{t}Bu). ^{13}C{^{1}H} NMR (THF-d_8, δ): 169.8, 164.4, 149.4, 128.9, 128.6, 124.9, 120.9, 120.1, 114.9 (each a s, ^{t}bpy and phenoxy carbons), 36.8 {s, ^{t}Bu-*C*(CH$_3$)$_3$}, 30.4 {s, ^{t}Bu-C(*C*H$_3$)$_3$}. Anal. Calcd for $C_{30}H_{34}N_2O_2Pt$: C, 55.46; H, 5.27; N, 4.31. Found: C, 54.85; H, 5.57; N, 3.76.

(^{t}bpy)Pt(Me)$_2$(I)$_2$ (8). In a round-bottom flask, (^{t}bpy)Pt(Me)$_2$ (0.069 g, 0.14 mmol) and iodine (0.038 g, 0.15 mmol) were combined in ∼15 mL of benzene. After stirring for 18 h, the solvent was removed in vacuo and the product was dried (0.082 g, 73% yield). A crystal suitable for an X-ray diffraction study was grown by slow diffusion of a THF solution layered with pentane. ^{1}H NMR (C_6D_6, δ): 8.34 (d, 2H, $^3J_{H5-H6}$ = 6 Hz, ^{t}bpy 6/6′), 7.94 (d, 2H, $^4J_{H3-H5}$ = 2 Hz, ^{t}bpy 3/3′), 6.76 (dd, 2H, $^3J_{H5-H6}$ = 6, $^4J_{H3-H5}$ = 2 Hz, ^{t}bpy 5/5′), 2.63 (s with Pt satellites, 6H, $^2J_{Pt-H}$ = 73 Hz, Pt−C*H*$_3$), 1.04 (s, 18H, ^{t}bpy ^{t}Bu). ^{13}C NMR ($CDCl_3$, δ): 164.0, 154.9, 147.7, 124.4, 120.5 (each a s, ^{t}bpy aryl resonances), 35.7 {s, ^{t}Bu-*C*(CH$_3$)$_3$}, 30.7 {s, ^{t}Bu-C(*C*H$_3$)$_3$}, −14.7 (s with Pt satellites, $^1J_{Pt-C}$ = 506 Hz, Pt-*C*H$_3$). Anal. Calcd for $C_{20}H_{30}I_2N_2Pt$: C, 32.14; H, 4.05; N, 3.75. Found: C, 32.38; H, 4.01; N, 3.70.

(^{t}bpy)Pt(Ph)$_2$(I)$_2$ (9). (^{t}bpy)Pt(Ph)$_2$ (0.137 g, 0.221 mmol) and iodine (0.061 g, 0.24 mmol) were combined in ∼20 mL of benzene in a round-bottom flask. After stirring for 12 h, the volatiles were reduced in vacuo to ∼1 mL. The addition of hexanes yielded an orange precipitate, which was filtered through a plug of silica gel on a fine-porosity frit. The solid was rinsed with 25% Et$_2$O/75% hexanes (v:v 3 × 3 mL) to remove excess iodine followed by methylene chloride to elute the orange complex from the silica gel. The filtrate was reduced to dryness in vacuo to yield an orange solid (0.161 g, 84% yield). ^{1}H NMR (C_6D_6, δ): 9.12 (d, 2H, $^3J_{H5-H6}$ = 6 Hz, ^{t}bpy 6/6′), 8.71 (d, 4H, $^3J_{HH}$ = 8 Hz, phenyl-*ortho*), 7.81 (d, 2H, $^4J_{H3-H5}$ = 2 Hz, ^{t}bpy 3/3′), 7.2−7.1 (m, 6H, overlapping phenyl-*meta* and -*para*), 6.47 (dd, 2H, $^3J_{H5-H6}$ = 6 Hz, $^4J_{H3-H5}$ = 2 Hz, ^{t}bpy 5/5′), 0.89 (s, 18H, ^{t}bpy ^{t}Bu). ^{13}C{^{1}H} NMR (C_6D_6, δ): 163.9, 155.9, 151.5, 146.2, 127.7, 126.8, 125.4, 124.3, 120.4 (each a s, ^{t}bpy and phenyl carbons), 35.2 {s, ^{t}bpy-*C*(CH$_3$)$_3$}, 30.3 {s, ^{t}bpy-C(*C*H$_3$)$_3$}. Anal. Calcd for $C_{30}H_{34}I_2N_2Pt$: C, 41.35; H, 3.93; N, 3.21. Found: C, 41.17; H, 3.83; N, 3.23.

(^{t}bpy)Pt(Me)$_2$(NHPh)(I) (10). In a round-bottom flask, (^{t}bpy)-Pt(Me)(NHPh) (**2**) (0.112 g, 0.196 mmol) and iodomethane (15 μL, 0.240) were combined in ∼15 mL of benzene. After stirring for 2 h, a color change from green to brown was observed, and the volatiles were reduced in vacuo to ∼1 mL. Hexanes were added to precipitate a brown

solid. The solid was collected by filtration on a fine-porosity frit and washed with hexanes (2 × 3 mL) and pentane (2 × 3 mL) (0.095 g, 68% yield). ^{1}H NMR (C_6D_6, δ): 9.67, 8.51 (each a d, each 1H, $^3J_{H5-H6}$ = 6 Hz, ^{t}bpy 6/6′), 7.78, 7.74 (each a br s, each 1H, ^{t}bpy 3/3′), 7.4−7.2 (overlapping *ortho*- and *meta*-anilido, 4H), 7.0−6.9 (overlapping *para*-anilido and ^{t}bpy5/5′, 2H), 6.72 (dd, 1H, $^3J_{H5-H6}$ = 6 Hz, $^4J_{H3-H5}$ = 2 Hz, ^{t}bpy 5/5′), 4.77 (br s with Pt satellites, 1H, $^2J_{Pt-H}$ = 50 Hz, Pt−N*H*Ph), 2.24 (s with Pt satellites, 3H, $^2J_{Pt-H}$ = 70 Hz, Pt−CH_3), 1.35 (s with Pt satellites, 3H, $^2J_{Pt-H}$ = 70 Hz, Pt−CH_3), 0.98, 0.95 (each a s, each 9H, ^{t}bpy ^{t}Bu). ^{13}C{^{1}H} NMR (C_6D_6, δ): 163.6, 157.2, 156.2, 153.6, 149.0, 148.8, 129.5, 125.0, 124.6, 122.6, 120.4, 119.7, 117.6 (each a s, ^{t}bpy aryl and anilido-phenyl carbons, one signal missing presumably due to coincidental overlap), 35.5, 35.4 {each a s, ^{t}Bu-*C*(CH$_3$)$_3$}, 30.5, 30.3 {each a s, ^{t}Bu-C(*C*H$_3$)$_3$}, 13.8 (s with Pt satellites, $^1J_{Pt-C}$ = 630 Hz, Pt-*C*H$_3$), −0.4 (s with Pt satellites, $^1J_{Pt-C}$ = 642 Hz, Pt-*C*H$_3$). Anal. Calcd for $C_{26}H_{36}IN_3Pt$: C, 43.82; H, 5.09; N, 5.90. Found: C, 43.54; H, 5.02; N, 5.63.

(^{t}bpy)Pt(Me)(C≡CPh) (11). (^{t}bpy)Pt(Me)(NHPh) (**2**) (0.061 g, 0.11 mmol) and phenylacetylene (12 μL, 0.11 mmol) were combined in ∼5 mL of benzene in a thick-walled glass pressure tube. The homogeneous blue-green solution was heated at 80 °C for 12 h in a temperature-controlled oil bath. The resulting orange solution was allowed to cool to room temperature, and the volatiles were reduced in vacuo to ∼1 mL. The addition of hexanes resulted in the formation of an orange precipitate. The solid was collected by filtration through a fine-porosity frit and washed with hexanes (3 × 2 mL) (0.041 g, 66% yield). ^{1}H NMR (C_6D_6, δ): 9.58, 8.65 (each a d, each 1H, $^3J_{H5-H6}$ = 6 Hz, ^{t}bpy 6/6′), 7.92 (d, 2H, $^3J_{HH}$ = 8 Hz, phenylacetylide-*ortho*), 7.64, 7.58 (each a d, each 1H, $^4J_{H3-H5}$ = 2 Hz, ^{t}bpy 3/3′), 7.26 (t, 2H, $^3J_{HH}$ = 7 Hz, phenylacetylide-*meta*), 7.08 (t, 1H, $^3J_{HH}$ = 8 Hz, phenylacetylide-*para*), 6.72, 6.55 (each a dd, each 1H, $^3J_{H5-H6}$ = 6 Hz, $^4J_{H3-H5}$ = 2 Hz, ^{t}bpy 5/5′), 1.65 (s with Pt satellites, 3H, $^2J_{Pt-H}$ = 81 Hz, Pt−CH_3), 1.10, 1.01 (each a s, each 9H, ^{t}bpy ^{t}Bu). ^{13}C{^{1}H} NMR (C_6D_6, δ): 161.3, 160.6, 158.4, 155.5, 150.5, 146.9, 132.7, 125.0, 124.6, 124.2, 120.0, 118.8 (each a s, ^{t}bpy aryl and acetylide-phenyl resonances, two signals missing presumably due to coincidental overlap), 103.0, 100.6 (each a s, C≡C carbons), 35.6, 35.5 {overlapping singlets, ^{t}Bu-*C*(CH$_3$)$_3$}, 30.3 {s, ^{t}Bu-C(*C*H$_3$)$_3$, one signal missing presumably to coincidental overlap}, −17.4 (s, Pt-*C*H$_3$). Note: Anticipated $^1J_{Pt-C}$ satellites were not observed due to a low signal-to-noise ratio. Anal. Calcd for $C_{27}H_{32}N_2Pt$: C, 55.95; H, 5.56; N, 4.83. Found: C, 55.68; H, 5.48; N, 4.71.

[(^{t}bpy)Pt(NHPh)(py)][BAr′$_4$] (12). (^{t}bpy)Pt(NHPh)$_2$ (**4**) (0.048 g, 0.074 mmol) and neat pyridine (∼20 equiv) were combined in a thick-walled glass pressure tube. After addition of HBAr′$_4$ (0.075 g, 0.074 mmol) the tube was sealed with a Teflon screw cap and the mixture was heated at 80 °C for ∼40 h in a temperature-controlled oil bath. Upon cooling to room temperature, the volatiles were removed in vacuo. After reconstitution in 5 mL of diethyl ether, the solution was transferred to a vial and the volatiles were removed in vacuo to yield a low-density brown solid (0.101 g, 91% yield). ^{1}H NMR (CD_2Cl_2, δ): 9.21 (d, 1H, $^3J_{H5-H6}$ = 6 Hz, ^{t}bpy 6/6′), 8.73 (dd, 1H, $^3J_{H5-H6}$ = 6 Hz, $^4J_{H3-H5}$ = 2 Hz, ^{t}bpy 5/5′), 8.10, 8.04 (each a d, each 1H, $^4J_{H3-H5}$ = 2 Hz, ^{t}bpy 3/3′), 7.96 (t, 1H, $^3J_{HH}$ = 8 Hz), 7.72 (br s, 8H, *ortho*-BAr′$_4$), 7.66 (dd, 1H, $^3J_{H5-H6}$ = 6 Hz, $^4J_{H3-H5}$ = 2 Hz, ^{t}bpy 5/5′), 7.55 (br s, 4H, *para*-BAr′$_4$), 7.50 (t, 2H, $^3J_{HH}$ = 8 Hz), 6.93−6.80 (m, 7H), 6.37 (t, 1H, $^3J_{HH}$ = 8 Hz), 2.90 (br s, 1H, anilido-N*H*), 1.45, 1.41 (each a s, each 9H, ^{t}bpy ^{t}Bu). ^{13}C{^{1}H} NMR (CD_2Cl_2, δ): 166.9, 166.8, 158.2, 157.0, 156.9, 153.6, 151.2, 148.4, 140.5, 129.6, 127.7, 125.9, 125.2, 120.9, 120.4, 116.7, 114.6 (each a s, ^{t}bpy, pyridine, and NH-phenyl carbons), 162.3 (q, $^1J_{B-C}$ = 50 Hz, *ipso*-BAr′$_4$), 135.4 (s, *ortho*-BAr′$_4$), 129.4 (q, $^2J_{C-F}$ = 31 Hz, *meta*-BAr′$_4$), 125.1 (q, $^1J_{C-F}$ = 271 Hz, *C*F$_3$−BAr′$_4$), 118.0 (s, *para*-BAr′$_4$), 36.6 {s, ^{t}Bu-*C*(CH$_3$)$_3$, one signal missing presumably due to coincidental overlap}, 30.4, 30.3 (each a s, ^{t}Bu-C(*C*H$_3$)$_3$). ^{19}F NMR (282.2 MHz, CD_2Cl_2, δ): −63.4 (s, BAr′$_4$ C*F*$_3$). Anal. Calcd for $C_{61}H_{47}BF_{24}N_4Pt$: C, 48.91; H, 3.16; N, 3.74. Found: C, 48.49; H, 3.01; N, 3.70.

[(^{t}bpy)Pt(OPh)(py)][BAr′$_4$] (13). In a round-bottom flask, (^{t}bpy)Pt(OPh)$_2$ (**7**) (0.051 g, 0.079 mmol) and pyridine (30 μL, 0.40 mmol) were combined in methylene chloride to give a green solution. HBAr′$_4$ was added, and the solution instantly turned gold. The reaction was stirred for 12 h, and the volatiles were removed in vacuo. After reconstitution in 5 mL of diethyl ether, the solution was transferred to a vial. The volatiles were removed to yield a low-density dark gold solid (0.098 g, 81%). ^{1}H NMR (CD_2Cl_2, δ): 8.82 (dd, 1H, $^3J_{H5-H6}$ = 6 Hz, $^4J_{H3-H5}$ = 2 Hz, ^{t}bpy 5/5′), 8.79 (d, 1H, $^3J_{H5-H6}$ = 6 Hz, ^{t}bpy 6/6′), 8.06, 8.04 (each a d, each 1H, $^4J_{H3-H5}$ = 2 Hz, ^{t}bpy 3/3′), 7.98 (t, 1H, $^3J_{HH}$ = 8 Hz, OPh or py *para*), 7.77 (d, 1H, $^3J_{H5-H6}$ = 6 Hz, ^{t}bpy 6/6′), 7.74−7.66 (m, 10H, overlapping *ortho*-BAr′$_4$ and OPh or py *ortho*), 7.57−7.47 (m, 7H, overlapping *para*-BAr′$_4$, ^{t}bpy 5/5′, and OPh or py *ortho*), 7.08−6.92 (m, 4H, overlapping OPh and py *meta*), 6.57 (t, 1H, $^3J_{HH}$ = 8 Hz, OPh or py *para*), 1.45, 1.42 (each a s, each 9H, ^{t}bpy ^{t}Bu). ^{13}C NMR (pyridine-d_5, δ): 168.1, 167.0, 166.4, 157.6, 157.0, 149.1, 130.0, 129.4, 125.7, 124.9, 122.5, 121.8, 120.8, 119.8, 118.9, 118.6, 117.8 (each a s, ^{t}bpy, pyridine, and phenoxide-phenyl carbons), 163.0 (q, $^1J_{B-C}$ = 50 Hz, *ipso*-BAr′$_4$), 134.4 (s, *ortho*-BAr′$_4$), 130.2 (q, $^2J_{C-F}$ = 31 Hz, *meta*-BAr′$_4$), 125.4 (q, $^1J_{C-F}$ = 271 Hz, *C*F$_3$−BAr′$_4$), 117.5 (s, *para*-BAr′$_4$), 36.5 {s, ^{t}Bu-*C*(CH$_3$)$_3$, one signal missing presumably due to coincidental overlap}, 30.1, 30.0 (each a s, ^{t}Bu-C(*C*H$_3$)$_3$). ^{19}F NMR (pyridine-d_5, δ): −62.2 (s, BAr′$_4$ C*F*$_3$). Satisfactory elemental analysis data were not obtained. Representative NMR spectra are provided in the Supporting Information.

[(^{t}bpy)Pt(μ-NHPh)]$_2$[BAr′$_4$]$_2$ (14). In a round-bottom flask, (^{t}bpy)Pt(NHPh)(Cl) (**5**) (0.063 g, 0.106 mmol) and AgBAr′$_4$ (0.106 g, 0.109 mmol) were combined in THF (∼15 mL), resulting in a homogeneous blue-green solution. After stirring for 48 h, the volatiles were removed in vacuo. Reconstitution in THF and filtration through Celite resulted in a brown filtrate that was reduced in vacuo to ∼1 mL. Hexanes were added, and the resulting brown solid was collected on a fine-porosity frit and washed with pentane (2 × 3 mL) (0.136 g, 58% yield). ^{1}H NMR (CD_2Cl_2, δ): 7.93 (d, 4H, $^3J_{HH}$ = 8 Hz, anilido-*ortho*), 7.90 (d, 4H, $^4J_{H3-H5}$ = 2 Hz, ^{t}bpy 3/3′), 7.85 (d, 4H, $^3J_{H5-H6}$ = 6 Hz, ^{t}bpy 6/6′), 7.72 (br s, 16H, *ortho*-BAr′$_4$), 7.54 (br s, 8H, *para*-BAr′$_4$), 7.44 (d, 4H, $^3J_{H5-H6}$ = 6 Hz, $^4J_{H3-H5}$ = 2 Hz, ^{t}bpy 5/5′), 7.36 (t, 4H, $^3J_{HH}$ = 8 Hz, anilido-*meta*), 7.19 (t, 2H, $^3J_{HH}$ = 8 Hz, anilido-*para*), 3.83 (br s, 2H, Pt−N*H*Ph), 1.33 (s, 36H, ^{t}bpy ^{t}Bu). ^{13}C{^{1}H} NMR (CD_2Cl_2, δ): 168.0, 156.6, 149.1, 148.4, 130.8, 127.0, 125.0, 124.5, 120.9 (each a s, ^{t}bpy and anilido-phenyl carbons), 162.3 (q, $^1J_{B-C}$ = 50 Hz, *ipso*-BAr′$_4$), 135.4 (s, *ortho*-BAr′$_4$), 129.4 (q, $^2J_{C-F}$ = 31 Hz, *meta*-BAr′$_4$), 125.1 (q, $^1J_{C-F}$ = 272 Hz, *C*F$_3$−BAr′$_4$), 118.0 (s, *para*-BAr′$_4$), 36.6 (s, ^{t}Bu-*C*(CH$_3$)$_3$), 30.2 (s, ^{t}Bu-C(*C*H$_3$)$_3$). ^{19}F{^{1}H} NMR (CD_2Cl_2, δ): −63.2 (BAr′$_4$-C*F*$_3$). Satisfactory elemental analysis data were not obtained. Representative NMR spectra are provided in the Supporting Information.

Kinetic Study of (^{t}bpy)Pt(Me)(NHPh) (2) and Phenylacetylene. Note: to ensure reproducibility, each kinetic experiment was performed in triplicate. A representative procedure is given. A screw-cap NMR tube was charged with 0.45 mL of C_6D_6, complex **2** (0.006 mmol, 0.0138 M), and hexamethylbenzene (5.9 × 10^{-4} mmol, 0.0013 M) as an internal standard. An initial ^{1}H NMR spectrum was acquired. Phenylacetylene (5.5 μL, 0.04 mmol) was added to the tube via microsyringe. The tube was placed in a ^{1}H NMR probe that was preheated to 80 °C. The reaction was monitored by ^{1}H NMR spectroscopy. The rate of reaction was determined by monitoring the disappearance of complex **2** (the resonance at 9.37 ppm was used). A linear plot of [**2**] versus time revealed a zero-order dependence on **2**. A representative plot is shown in Figure 8. A plot of k_{obs} versus phenylacetylene equivalents is shown in Figure 9.

Kinetic study of the Reaction between (^{t}bpy)Pt(Me)(NHPh) (2) and Phenylacetylene with Catalytic [(^{t}bpy)Pt(Me)(NH$_2$Ph)][TFA] (1). Note: to ensure reproducibility, each kinetic

experiment was performed in triplicate. A representative procedure is given. A vial was charged with a solution of complex **1** in diethyl ether (51.8 μL, 5.59×10^{-4} mmol), and diethyl ether was removed in vacuo in order to obtain an accurate concentration. The vial was then charged with 0.45 mL of C_6D_6, complex **2** (5.59×10^{-3} mmol, 0.0124 M), and hexamethylbenzene (6.6×10^{-4} mmol, 0.0014 M). The solution was added to a screw-cap NMR tube, and phenylacetylene (12.3 μL, 0.129 mmol) was added to the tube via microsyringe. The tube was placed in a ^{1}H NMR probe that was preheated to 80 °C. The reaction was monitored by ^{1}H NMR spectroscopy. The rate of reaction was determined by monitoring the disappearance of complex **2** (the resonance at 9.37 ppm was used). A plot of k_{obs} versus equivalents of complex **1** reveals a first-order dependence (Figure 10).

Reaction of (^{t}bpy)Pt(Me)(NHPh) (2) and H_2. A J. Young NMR tube was charged with (^{t}bpy)Pt(Me)(NHPh) (**2**) (0.006 g, 0.011 mmol), a small crystal of hexamethylbenzene (as internal standard), and C_6D_6 (0.5 mL). An initial ^{1}H NMR spectrum was acquired. After degassing the solution with three freeze−pump−thaw cycles, the tube was charged with H_2 (~45 psi). The solution was monitored by ^{1}H NMR spectroscopy. After 7 h at room temperature, a new Pt−methyl resonance at 2.21 ppm (s with Pt satellites, $^2J_{Pt-H} = 83$ Hz) was observed (by ^{1}H NMR spectroscopy) along with a Pt−hydride resonance at −14.8 ppm (s with Pt satellites, $^1J_{Pt-H}$ = 1575 Hz). In addition, resonances due to ^{t}bpy of a new Pt complex were observed as well as resonances due to free aniline. These data are consistent with the formation of (^{t}bpy)Pt(Me)(H) and NH_2Ph. After 12 h, complete conversion to free aniline, free methane, and free ^{t}bpy was observed. In addition, a black precipitate was observed, which we presume is Pt(s).

Kinetic Studies of (^{t}bpy)Pt(Me)(NHPh) (2) and H_2. Note: to ensure reproducibility, each kinetic experiment was performed a minimum of three times. A representative procedure is given. A thick-walled high-pressure NMR tube with a Teflon valve was charged with 0.3 mL of C_6D_6, complex **2** (0.004 mmol, 0.0138 M), and hexamethylbenzene (0.0004 mmol, 0.00131 M, as internal standard). An initial ^{1}H NMR spectrum was acquired. After degassing the solution with three freeze−pump−thaw cycles, the tube was charged with H_2 (~200 psi). The reaction was monitored by ^{1}H NMR spectroscopy every 10 min until complete conversion to free aniline, methane, and ^{t}bpy was observed. The rate of reaction was determined by monitoring the disappearance of complex **2** (the resonance at 9.37 ppm was used). A plot of [**2**] versus time revealed an initial induction period and a sigmoidal fit (Figure 11, plot A).

Mercury Test. A thick-walled high-pressure NMR tube with a Teflon valve was charged with 0.1 mL of C_6D_6, complex **2** (0.0014 mmol, 0.0139 M), hexamethylbenzene (0.00016 mmol, 0.00162 M, as internal standard), and a drop of elemental Hg. An initial ^{1}H NMR spectrum was acquired. After degassing the solution with three freeze−pump−thaw cycles, the tube was charged with H_2 (~200 psi). The reaction was monitored by ^{1}H NMR spectroscopy every 20 min for ~7 h (Figure 11, plot B). There was virtually no change in the concentration of complex **2**.

Reaction of Complex 2 and H_2 in the Presence of "Generated" Pt(s). A high-pressure NMR tube was charged with 0.1 mL of C_6D_6, complex **2** (0.0014 mmol, 0.0139 M), and hexamethylbenzene (0.00016 mmol, 0.00162 M, as internal standard). An initial ^{1}H NMR spectrum was acquired. After degassing the solution with three freeze−pump−thaw cycles, the tube was charged with H_2 (~200 psi). The mixture was allowed to react for ~3 h, at which time the formation of Pt(s) was visible and initial conversion to (^{t}bpy)Pt(Me)(H) was evident. The solution was carefully decanted, and the tube was rinsed with C_6D_6 leaving Pt(s) on the walls. The same NMR tube was charged with 0.1 mL of fresh complex **2**/hexamethylbenzene/C_6D_6 solution. Again, the solution was degassed with three freeze−pump−thaw cycles and charged with H_2 (~200 psi). The reaction was monitored by ^{1}H NMR spectroscopy every 10 min for ~3 h. A plot of [**2**] versus time revealed conversion of **2** and H_2 indicative of a reaction with a zero-order dependence on complex **2** (Figure 11, plot C).

Filtration Test. A thick-walled high-pressure NMR tube with a Teflon valve was charged with 0.45 mL of C_6D_6, complex **2** (0.0057 mmol, 0.0126 M), and hexamethylbenzene (0.0011 mmol, 0.00246 M, as internal standard). An initial ^{1}H NMR spectrum was acquired. After degassing the solution with three freeze−pump−thaw cycles, the tube was charged with H_2 (~200 psi). The reaction was monitored by ^{1}H NMR spectroscopy every 5 min for ~5 h through the induction period and initial stages of the reaction. After this time period, the solution was filtered through Celite to remove Pt(s). The filtrate was added to a new thick-walled high-pressure NMR tube with a Teflon valve, degassed with three freeze−pump−thaw cycles, and charged with H_2 (~200 psi). Monitoring by ^{1}H NMR spectroscopy was continued for ~2 h until the reaction was complete. A plot of [**2**] versus time for the filtered solution revealed a *second* induction period (Figure 11, plot D).

Reaction with Added Pt/C. A thick-walled high-pressure NMR tube with a Teflon valve was charged with 0.1 mL of C_6D_6, complex **2** (0.0057 mmol, 0.0126 M), hexamethylbenzene (0.0011 mmol, 0.00246 M, as internal standard), and Pt (10% by weight) on carbon (0.001 g). An initial ^{1}H NMR spectrum was acquired. After degassing the solution with three freeze−pump−thaw cycles, the tube was charged with H_2 (~ 200 psi). The reaction was ~50% complete after ~5 min and reached completion after ~1 h.

Reaction of [(^{t}bpy)Pt(Ph)(NC_5F_5)][BAr'_4] with Aniline and Phenol. In two separate experiments, [(^{t}bpy)Pt(Ph)(NC_5F_5)][BAr'_4] (0.007 g, 0.004 mmol) and 1 equiv of pyridine were combined with 5 equiv of either aniline or phenol in CD_2Cl_2 in a screw-cap NMR tube. An initial ^{1}H NMR spectrum was acquired. After heating the tubes to 100 °C in a temperature-controlled oil bath for 24 h, the ^{1}H NMR spectra revealed the formation of complexes **12** and **13** along with free benzene.

Computational Methods. All calculations were performed with the Gaussian 03 program suite[82] using the B3LYP density functional[83,84] in conjunction with the CEP-31G valence basis sets and pseudopotentials of Stevens et al.[85,86] augmented with a set of d-polarization functions for main group elements (exponents of 0.80 for C, N, and O and 0.55 for P). The -31G basis set was used for H atoms.

Optimized geometries and transition states (all studied species were singlet spin states) were verified by the presence of zero and one imaginary frequency, respectively, in the calculated energy Hessian. Thermochemistry was determined at 1 atm and 298.15 K using unscaled B3LYP/CEP-31G(d) frequencies.

■ ASSOCIATED CONTENT

Supporting Information. Computational details, NMR spectra, and X-ray crystallographic data files. This material is available free of charge via the Internet at http://pubs.acs.org.

■ AUTHOR INFORMATION

Corresponding Author
*E-mail: tbg7h@virginia.edu (T.B.G.), t@unt.edu (T.R.C.).

■ ACKNOWLEDGMENT

T.B.G. acknowledges the National Science Foundation (CHE-0848693) for financial support of this work. T.R.C. thanks the National Science Foundation for support (CHE-0701247) and facilities (CHE-0741936). A.W.P. thanks the UNT Toulouse Graduate School for a Dissertation Fellowship.

■ REFERENCES

(1) Bryndza, H. E.; Tam, W. *Chem. Rev.* **1988**, *88*, 1163–1188.
(2) Fulton, J. R.; Holland, A. W.; Fox, D. J.; Bergman, R. G. *Acc. Chem. Res.* **2002**, *35*, 44–56.

(3) Gunnoe, T. B. *Eur. J. Inorg. Chem.* **2007**, 1185–1203.
(4) Sharp, P. R. *Comments Inorg. Chem.* **1999**, *21*, 85–114.
(5) Lappert, M. F.; Power, P. P.; Protchenko, A. V.; Seeber, A. L. *Metal Amide Chemistry*; John Wiley & Sons, Ltd.: West Sussex, 2009.
(6) Wolfe, J. P.; Wagaw, S.; Marcoux, J.-F.; Buchwald, S. L. *Acc. Chem. Res.* **1998**, *31*, 805–818.
(7) Roundhill, D. M. *Catal. Today* **1997**, *37*, 155–165.
(8) Müller, T. E.; Beller, M. *Chem. Rev.* **1998**, *98*, 675–703.
(9) Bergman, R. G. *Polyhedron* **1995**, *14*, 3227–3237.
(10) Sharp, P. R. *J. Chem. Soc., Dalton Trans.* **2000**, 2647–2657.
(11) Hartwig, J. F. *Nature* **2008**, *455*, 314–322.
(12) Feng, Y.; Lail, M.; Foley, N. A.; Gunnoe, T. B.; Barakat, K. A.; Cundari, T. R.; Petersen, J. L. *J. Am. Chem. Soc.* **2006**, *128*, 7982–7994.
(13) Feng, Y.; Lail, M.; Barakat, K. A.; Cundari, T. R.; Gunnoe, T. B.; Petersen, J. L. *J. Am. Chem. Soc.* **2005**, *127*, 14174–14175.
(14) Tenn, W. J., III; Young, K. J. H.; Bhalla, G.; Oxgaard, J.; Goddard, W. A., III; Periana, R. A. *J. Am. Chem. Soc.* **2005**, *127*, 14172–14173.
(15) Tenn, W. J., III; Young, K. J. H.; Oxgaard, J.; Nielson, R. J.; Goddard, W. A., III; Periana, R. A. *Organometallics* **2006**, *25*, 5173–5175.
(16) Hanson, S. K.; Heinekey, D. M.; Goldberg, K. I. *Organometallics* **2008**, *27*, 1454–1463.
(17) Cowan, R. L.; Trogler, W. C. *J. Am. Chem. Soc.* **1989**, *111*, 4750–4761.
(18) Holland, P. L.; Andersen, R. A.; Bergman, R. G. *Comments Inorg. Chem.* **1999**, *21*, 115–129.
(19) Fulton, J. R.; Sklenak, S.; Bouwkamp, M. W.; Bergman, R. G. *J. Am. Chem. Soc.* **2002**, *124*, 4722–4737.
(20) Jayaprakash, K. N.; Conner, D.; Gunnoe, T. B. *Organometallics* **2001**, *20*, 5254–5256.
(21) Fox, D. J.; Bergman, R. G. *Organometallics* **2004**, *23*, 1656–1670.
(22) Ess, D. H.; Gunnoe, T. B.; Cundari, T. R.; Goddard, W. A., III; Periana, R. A. *Organometallics* **2010**, *29*, 6801–6815.
(23) Webb, J. R.; Bolaño, T. B.; Gunnoe, T. B. *ChemSusChem* **2011**, *4*, 37–49.
(24) Webb, J. R.; Pierpont, A. W.; Munro-Leighton, C.; Gunnoe, T. B.; Cundari, T. R.; Boyle, P. D. *J. Am. Chem. Soc.* **2010**, *132*, 4520–4521.
(25) Hill, G. S.; Rendina, L. M.; Puddephatt, R. J. *J. Chem. Soc., Dalton Trans.* **1996**, 1809–1813.
(26) Albéniz, A. C.; Calle, V.; Espinet, P.; Gómez, S. *Inorg. Chem.* **2001**, *40*, 4211–4216 and references therein..
(27) Khusnutdinova, J. R.; Zavalij, P. Y.; Vedernikov, A. N. *Can. J. Chem.* **2009**, *87*, 110–120.
(28) Radlowski, C. A.; Liu, C. F.; Jun, M. J. *Inorg. Chim. Acta* **1984**, *86*, 101–106.
(29) Kapteijn, G. M.; Meijer, M. D.; Grove, D. M.; Veldman, N.; Spek, A. L.; van Koten, G. *Inorg. Chim. Acta* **1997**, *264*, 211–217.
(30) Jawad, J. K.; Adams, H.; Morris, M. J. *Inorg. Chim. Acta* **2010**, *363*, 685–690.
(31) Achar, S.; Scott, J. D.; Vittal, J. J.; Puddephatt, R. J. *Organometallics* **1993**, *12*, 4592–4598.
(32) Osakada, K.; Kim, Y.-J.; Yamamoto, A. *J. Organomet. Chem.* **1990**, *382*, 303–317.
(33) Frank, W.; Heck, L.; Müller-Becker, S.; Raber, T. *Inorg. Chim. Acta* **1997**, *265*, 17–22.
(34) Kretschmer, V. M.; Heck, L. *Z. Anorg. Allg. Chem.* **1982**, *490*, 215–229.
(35) Klein, V. B.; Heck, L. *Z. Anorg. Allg. Chem.* **1975**, *416*, 269–284.
(36) Harkins, S. B.; Peters, J. C. *Inorg. Chem.* **2006**, *45*, 4316–4318.
(37) Pawlikowski, A. V.; Getty, A. D.; Goldberg, K. I. *J. Am. Chem. Soc.* **2007**, *129*, 10382–10393.
(38) Munro-Leighton, C.; Feng, Y.; Zhang, J.; Alsop, N. M.; Gunnoe, T. B.; Boyle, P. D.; Petersen, J. L. *Inorg. Chem.* **2008**, *47*, 6124–6126.
(39) Achar, S.; Scott, J. D.; Puddephatt, R. J. *Organometallics* **1992**, *11*, 2325–2326.
(40) OReilly, S. A.; White, P. S.; Templeton, J. L. *J. Am. Chem. Soc.* **1996**, *118*, 5684–5689.
(41) Kelly, M. E.; Gomez-Ruiz, S.; Kluge, R.; Merzweiler, K.; Steinborn, D.; Wagner, C.; Schmidt, H. *Inorg. Chim. Acta* **2009**, *362*, 1323–1332.
(42) Goldberg, K. I.; Goldman, A. S. *Activation and Functionalization of C-H Bonds*; American Chemical Society: Washington, DC, 2004; Vol. 885.
(43) Hoyt, H. M.; Michael, F. E.; Bergman, R. G. *J. Am. Chem. Soc.* **2004**, *126*, 1018–1019.
(44) Bennett, J. L.; Wolczanski, P. T. *J. Am. Chem. Soc.* **1994**, *116*, 2179–2180.
(45) Cummins, C. C.; Baxter, S. M.; Wolczanski, P. T. *J. Am. Chem. Soc.* **1988**, *110*, 8731–8733.
(46) With, J. D.; Horton, A. D. *Angew. Chem., Int. Ed. Engl.* **1993**, *32*, 903–905.
(47) Schaller, C. P.; Wolczanski, P. T. *Inorg. Chem.* **1993**, *32*, 131–144.
(48) Oxgaard, J.; Tenn, I.; W., J.; Nielson, R. J.; Periana, R. A.; Goddard, W. A., III *Organometallics* **2007**, *26*, 1565–1567.
(49) Bercaw, J. E.; Hazari, N.; Labinger, J. A. *Organometallics* **2009**, *28*, 5489–5492.
(50) Cundari, T. R.; Grimes, T. V.; Gunnoe, T. B. *J. Am. Chem. Soc.* **2007**, *129*, 13172–13182.
(51) Abdur-Rashid, K.; Fong, T. P.; Greaves, B.; Gusev, D. G.; Hinman, J. G.; Landau, S. E.; Lough, A. J.; Morris, R. J. *J. Am. Chem. Soc.* **2000**, *122*, 9155–9171.
(52) Bordwell, F. G. *Acc. Chem. Res.* **1988**, *21*, 456–463.
(53) Conner, D.; Jayaprakash, K. N.; Wells, M. B.; Manzer, S.; Gunnoe, T. B.; Boyle, P. D. *Inorg. Chem.* **2003**, *42*, 4759–4772.
(54) Holland, A. W.; Bergman, R. G. *J. Am. Chem. Soc.* **2002**, *124*, 14684–14695.
(55) Goj, L. A.; Blue, E. D.; Delp, S. A.; Gunnoe, T. B.; Cundari, T. R.; Pierpont, A. W.; Petersen, J. L.; Boyle, P. D. *Inorg. Chem.* **2006**, *45*, 9032–9045.
(56) Munro-Leighton, C.; Blue, E. D.; Gunnoe, T. B. *J. Am. Chem. Soc.* **2006**, *128*, 1446–1447.
(57) Munro-Leighton, C.; Delp, S. A.; Blue, E. D.; Gunnoe, T. B. *Organometallics* **2007**, *26*, 1483–1493.
(58) Zhang, Y. G. *Inorg. Chem.* **1982**, *21*, 3886–3889.
(59) Belluco, U.; Bertani, R.; Meneghetti, F.; Michelin, R. A.; Mozzon, M. *J. Organomet. Chem.* **1999**, *583*, 131–135.
(60) Boutadla, Y.; Davies, D. L.; Macgregor, S. A.; Poblador-Bahamonde, A. I. *Dalton Trans.* **2009**, *30*, 5820–5831.
(61) Wick, D. D.; Goldberg, K. I. *J. Am. Chem. Soc.* **1997**, *119*, 10235–10236.
(62) Johansson, L.; Ryan, O. B.; Romming, C.; Tilset, M. *J. Am. Chem. Soc.* **2001**, *123*, 6579–6590.
(63) Zhong, H. A.; Labinger, J. A.; Bercaw, J. E. *J. Am. Chem. Soc.* **2002**, *124*, 1378–1399.
(64) Heiden, Z. M.; Rauchfuss, T. B. *J. Am. Chem. Soc.* **2006**, *128*, 13048–13049.
(65) Sandoval, C. A.; Ohkuma, T.; Muñiz, K.; Noyori, R. *J. Am. Chem. Soc.* **2003**, *125*, 13490–13503.
(66) Fryzuk, M. D.; Montgomery, C. D.; Rettig, S. J. *Organometallics* **1991**, *10*, 467–473.
(67) Fulmer, G. R.; Muller, R. P.; Kemp, R. A.; Goldberg, K. I. *J. Am. Chem. Soc.* **2009**, *131*, 1346–+.
(68) Conner, D.; Jayaprakash, K. N.; Cundari, T. R.; Gunnoe, T. B. *Organometallics* **2004**, *23*, 2724–2733.
(69) Yang, J. Y.; Bullock, R. M.; Shaw, W. J.; Twamley, B.; Fraze, K.; DuBois, M. R.; DuBois, D. L. *J. Am. Chem. Soc.* **2009**, *131*, 5935–5945.
(70) Abdur-Rashid, K.; Faatz, M.; Lough, A. J.; Morris, R. H. *J. Am. Chem. Soc.* **2001**, *123*, 7473–7474.
(71) Widegren, J. A.; Finke, R. G. *J. Mol. Catal. A: Chem.* **2003**, *198*, 317–341.
(72) Hamlin, J. E.; Hirai, K.; Millan, A.; Maitlis, P. M. *J. Mol. Catal.* **1980**, *7*, 543–544.
(73) McKeown, B. A.; Foley, N. A.; Lee, J. P.; Gunnoe, T. B. *Organometallics* **2008**, *27*, 4031–4033.

(74) Miller, T. M.; Izumi, A. N.; Shih, Y. S.; Whitesides, G. M. *J. Am. Chem. Soc.* **1988**, *110*, 3146–3156.
(75) Begum, R. A.; Chanda, N.; Ramakrishna, T. V. V.; Sharp, P. R. *J. Am. Chem. Soc.* **2005**, *127*, 13494–13495.
(76) Luinstra, G. A.; Wang, L.; Stahl, S. S.; Labinger, J. A.; Bercaw, J. E. *J. Organomet. Chem.* **1995**, *504*, 75–91.
(77) Shilov, A. E.; Shulpin, G. B. *Russ. Chem. Rev.* **1987**, *56*, 442–464.
(78) Yakelis, N. A.; Bergman, R. G. *Organometallics* **2005**, *24*, 3579–3591.
(79) Brookhart, M.; Grant, B.; Volpe, A. F., Jr. *Organometallics* **1992**, *11*, 3920–3922.
(80) Miller, K. J.; Kitagawa, T. T.; Abu-Omar, M. M. *Organometallics* **2001**, *20*, 4403–4412.
(81) Ong, C. M.; Jennings, M. C.; Puddephatt, R. J. *Can. J. Chem.* **2003**, *81*, 1196–1205.
(82) Frisch, M. J.; ; Pople, J. A.; et al. *Gaussian 03*, Revision D.02; Gaussian Inc.: Wallingford, CT, 2004.
(83) Becke, A. D. *J. Chem. Phys.* **1993**, *98*, 1372–1377.
(84) Becke, A. D. *J. Chem. Phys.* **1993**, *98*, 5648–5652.
(85) Stevens, W. J.; Basch, H.; Krauss, M. *J. Chem. Phys.* **1984**, *81*, 6026–6033.
(86) Stevens, W. J.; Krauss, M.; Basch, H.; Jasien, P. G. *Can. J. Chem.* **1992**, *70*, 612–613.